Properties of Na_xCoO_2

by

Helia Jalili

B.Sc., Polytechnic University of Tehran, 2001

A THESIS SUBMITTED IN PARTIAL FULFILMENT OF
THE REQUIREMENTS FOR THE DEGREE OF

MASTER OF SCIENCE

in

The Faculty of Mathematics and Sciences

Department of Physics

BROCK UNIVERSITY

May 11, 2005

In presenting this thesis in partial fulfilment of the requirements for an advanced degree at the Brock University, I agree that the Library shall make it freely available for reference and study. I further agree that permission for extensive copying of this thesis for scholarly purposes may be granted by the head of my department or by his or her representatives. It is understood that copying or publication of this thesis for financial gain shall not be allowed without my written permission.

(Signature) _____

Department of Physics

Brock University
St.Catharines, Canada

Date _____

Abstract

Polycrystalline samples of Na_xCoO_2 were prepared using the "Rapid heat-up" method. One set of samples was annealed in flowing O_2, while the other set in flowing Argon. X-Ray diffraction measurements indicated a stable phase of $Na_{0.7}CoO_2$ mixed with Co_3O_4 for all the samples even though they differed in concentration of Na. Argon annealed samples were insulators, whereas the ones annealed in O_2 were metallic. Most of the measurements were performed on the sample $Na_{0.7}CoO_2$, because it is the host compound for the superconductor sample $Na_{0.35}CoO_2{\cdot}H_2O$. Magnetization measurement showed that the magnetic moment decreased with increasing sodium concentration. This is due to the existence of Co_3O_4 in samples with Na$\neq$ 0.7. As sodium concentration decreases, the magnetic moment increases due to the increasing concentration of Co_3O_4 and its large magnetic moment. Magnetization measurements showed that the magnetic moment of $Na_{0.7}CoO_2$ is field-dependent in low fields and field-independent in fields higher than 100 G. Resistivity changes with temperature ($d\rho/dT$) increased with increasing Na concentration. Also resistivity measurements were performed under different hydrostatic pressures on $Na_{0.7}CoO_2$. Two transitions were observed; one at a temperature T_1 $\simeq$20 K and the other at T_2 $\simeq$280 K, the transition at T_1 has a magnetic origin and the one at T_2 is a structural transition. It was noticed that pressure affects resistivity of the sample. At higher pressures resistivity changes faster with temperature. Magnetoresistance measurement showed a small change in the resistivity, especially at lower temperatures. A novel layered superconductor $Na_{0.35}CoO_2{\cdot}H_2O$ was prepared using de-intercalation of Na from the host compound $Na_{0.7}CoO_2$. From the temperature

dependence of the magnetization, the superconducting transition temperature and lower critical field have been estimated as T_C=4.12 K and H_{C1}=66 G, respectively.

Contents

List of Tables

List of Figures

Acknowledgements

It is a pleasure to thank the many people who made this thesis possible. First and foremost I would like to thank my Supervisor, Dr. F. Razavi for his insight, guidance and patience. He provided me with the freedom to do things in the way that I thought should be done. One could not simply wish for a better and friendlier adviser. My appreciation goes to my other committee members, Dr. Bose, Dr. Reedyk, Dr. Finn and the external examiner, Dr.Luke for reviewing this thesis, and for their guidance and assistance. I would also like to thank Dr. Sudhakar Rao for his time and his unlimited help on various parts of the thesis, numerous scientific discussions and his many constructive comments have greatly improved my work. I gratefully acknowledge the constant and invaluable academic and personal support received from all faculty members in the Physics department, Dr. Wiebe, Dr. Sternin, Dr. Crandles, Dr. Mitrovic and Dr. Samokhin. My gratitude to Fran and Irene for their endless patience and goodwill. I also thank the machine shop and electronic shop experts for their great job. I am grateful for the company of my friends. Thank you very much for being there for me.I am forever indebted to my family for their understanding, endless patience and encouragement when it was most required. I can only hope you are as proud of me as I am of you.
Finally, I would like to dedicate my thesis to my grandmother, my parents and my sister Kimia, this is for you.

Chapter 1

Introduction

The discovery of high T_c superconductors encouraged scientists to look for new materials that are interesting and technologically useful. In 1997, Terasaki *et al.* [1] reported large thermoelectric power and low resistivity in sodium cobalt oxide simultaneously, which enables this compound to become a promising candidate for thermoelectric applications.[1] The large magnitude of thermoelectric power, *i.e.* $S > 50\,\mu$V/K at 300 K and low resistivity (around $200\mu\Omega$·cm) of this compound is difficult to explain with conventional one electron pictures [1]. Cava and coworkers found that the magnetic susceptibility of $Na_{.68}CoO_2$ is surprisingly high. At 2 K it is 100 times larger than the susceptibility of the ordinary metals [2, 3]. Moreover, the temperature dependence of the susceptibility can be described by the Curie-Weiss relationship, which is characteristic of materials in which the spins are localized, unlike the spin in conventional metals, which are tied to delocalized electrons.

In March 2003, Takada [4], reported that $Na_xCoO_2{\cdot}yH_2O$ (x$\sim$0.35, y$\sim$1.3) is a superconductor with a T_c of about 5 K. This report made $Na_xCoO_2{\cdot}yH_2O$ even more interesting.

Na_xCoO_2 belongs to a bronze-type compound expressed as A_xBO_2, which was first identified by Jansen and Hoppe [1, 5]. In CoO_2, without Na, each cobalt atom is in the Co^{4+} valence state; five electrons occupy the 3 d orbitals, whose energy levels are sketched in Fig. 1.1. Only the outermost 3 d electron is unpaired, and Co^{+4} has a spin of 1/2. When Na atoms are added to this compound, each contributes one electron, thereby changing Co^{+4} to a spinless Co^{+3} state. The thermoelectric material, with x$\approx$0.7, has on average 30

[1] A thermoelectric device can convert heat into electric energy through the thermoelectric power of solids.

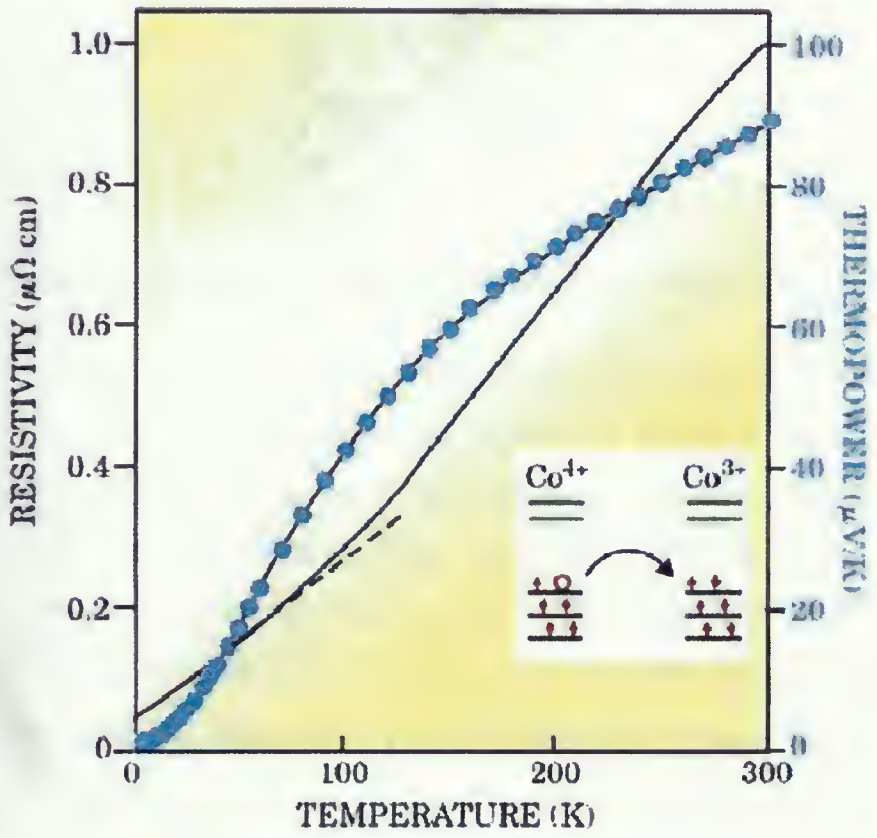

Figure 1.1: **Properties of sodium cobalt oxide as a function of temperature.** Resistivity (the black curve) behaves like that of most metals; whereas the thermopower (blue) is much higher. Inset: energy level occupied by the outer 3 d-electrons (red arrows) in Co^{+4} and Co^{+3} ions in Na_xCoO_2. Electrons donated by Na atoms change Co^{+4} atoms to Co^{+3}. A hole (open circle) can hop from one to the other, as sketched [3].

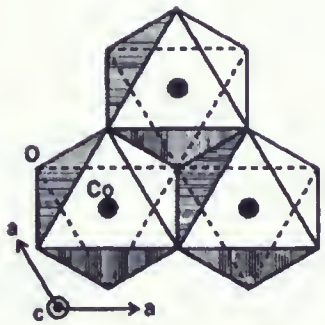

Figure 1.2: **Cobalt oxide layer**. The figure is reproduced from [1].

percent Co^{+4} and the rest is Co^{+3}. To make the superconducting form, Takada *et al.* [4] managed to coax more Na atoms to leave the material and thereby decrease the doping to x≈0.3. The lighter doping reverses the previous picture so that 70 percent of the sites are occupied by spins. As holes hop around, the spinless Co^{+3} ions appear to move in a sea of Co^{+4} sites, effectively becoming charge carriers with no spin. It has been reported [4] that the crystal structure of the superconducting $Na_xCoO_2{\cdot}(3/4)H_2O$ compound only differs from the parent compound $Na_{0.7}CoO_2$ by the intercalation of water molecules around the sodium ions to enlarge the CoO_2 layers and to reduce the sodium charges. The structure of $Na_xCoO_2{\cdot}(3/4)H_2O$ consists of 2-dimensional triangular CoO_2 (see Fig. 1.2) separated by a thick insulating layer of Na^+ ions and H_2O molecules Fig.(1.3).

Experimentalists are already trying to answer the question, "If adding Na is equivalent to electron doping, what role is played by the water, which so far is essential in achieving superconductivity?" Some theorists postulate that the water screens cobalt atoms from the strong coloumb force of the Na atoms [3]. $Na_xCoO_2{\cdot}yH_2O$ materials have structural similarity with high T_c copper oxides. An important similarity to high T_c superconductors is that Na_xCoO_2 is a layered transition-metal oxide as is schematically shown in Fig. 1.3, where Na and CoO_2 are alternately stacked along the c axis, so the physical properties are

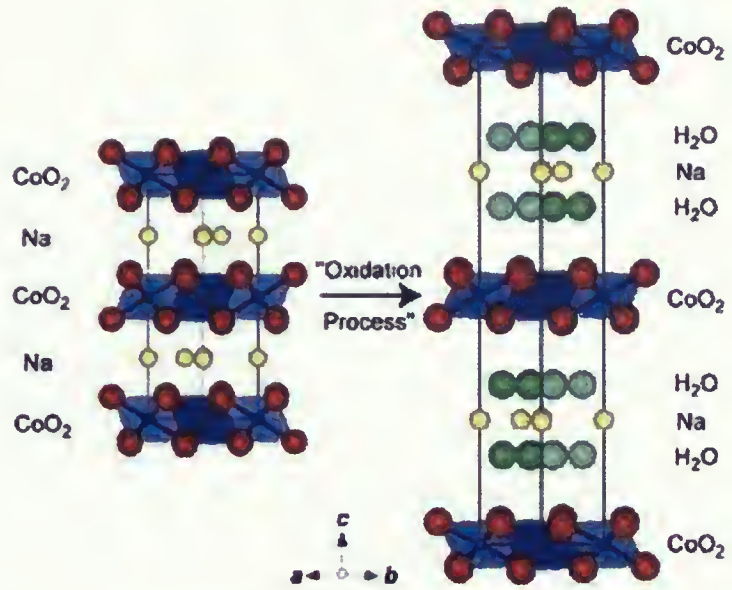

Figure 1.3: **Sodium Cobalt Oxide structure.** The figure is reproduced from [4].

expected to be highly two dimensional (2-D). However the CoO_2 layer is different in structure from the CuO_2 layer of HTC's. The former is a 2-D triangle lattice and the latter is a 2-D square lattice [1]. The structure of the Cobalt oxide layer is shown in Fig. 1.2.

Takada *et al.* [4] obtained a $Na_xCoO_2{\cdot}yH_2O$ sample through chemical oxidation of the parent compound $Na_{0.7}CoO_2$ [6]. $Na_{0.7}CoO_2$ has a hexagonal layered structure (space group $P6_3/mmc$) consisting of the 2-D layers of CoO_2 and charge balancing Na^+ ions (see Fig. 1.3). Fig. 1.4 shows an XRD (X-Ray Diffraction) pattern of the product obtained from oxidation. All the reflections were index matched on the basis of space group $P6_3/mmc$. A marked increase in "c-axis" was observed supporting the idea that the intercalation of certain "guest" molecules occurred in the oxidation process in addition to the de-intercalation of Na^+ ions. H_2O is the most probable candidate for the guest molecule. Rietveld analysis of the XRD data was carried out by adopting the structural model shown in Fig. 1.3. The Rietveld refinement patterns are shown in Fig. 1.4. The H_2O content resulting from this analysis came out to be 1.47 per formula unit [7]. The magnetic susceptibility of $Na_xCoO_2{\cdot}yH_2O$ is

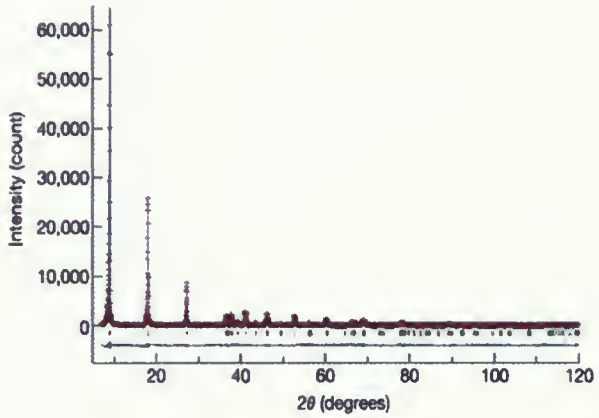

Figure 1.4: Rietveld refinement pattern for $Na_xCoO_2{\cdot}yH_2O$. The observed diffraction intensities are represented by red plus signs, and the calculated patterns by a green solid line. Short light green vertical bars below the observed and calculated patterns indicate the positions of allowed Bragg diffractions. The oxidation process slightly decreased the "a-axis" from $2.8292(3)°A$ for the parent compound to $2.8230(2)°A$, where the parentheses indicate standard deviations, probably because Co^{3+} ions where partially oxidized to smaller Co^{4+} ions. On the other hand, c increased dramatically from $10.9628(8)°A$ to $19.6207(14)°A$ [7].

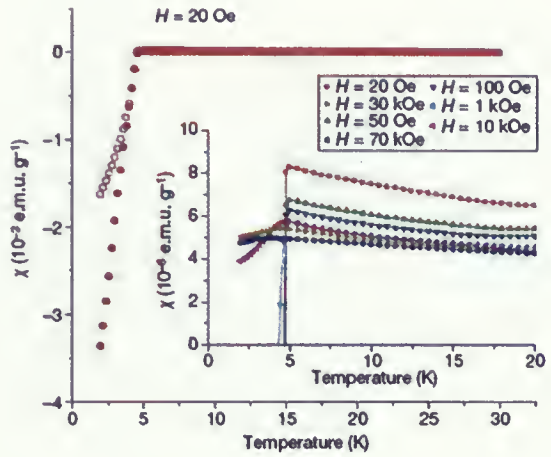

Figure 1.5: **Magnetic susceptibility (χ) of $Na_xCoO_2{\cdot}yH_2O$.** Filled circles indicate zero-field cooling; open circles indicate field cooling. The susceptibility is measured in the magnetic field of 20Oe. The inset shows χ measured under various magnetic fields by zero-field cooling process [7].

plotted in Fig. 1.5 as a function of temperature. A steep decrease of susceptibility is observed in the measurements under magnetic field $H = 20\ Oe$ at about 5 K both in zero-field cool (ZFC) and field cool (FC) processes [7].

From the susceptibility data, it can be concluded that the present phase undergoes a superconducting transition at about 5 K, because only superconductivity can account for such a large diamagnetism. Downturn of the susceptibility was still observed near 5 K even at 70 kOe, but the transition became quite broad and the susceptibility was not negative even at 2 K [7]. The electric resistivity (ρ) of the $Na_xCoO_2{\cdot}yH_2O$ is shown in Fig. 1.6. Zero resistivity was not obtained down to 2 K in the sample made by Takada *et al.* [4] because it was impossible to prepare a tightly sintered ceramic specimen [7]. The effect of hydrostatic pressure on the superconducting transition temperature of $Na_xCoO_2{\cdot}yH_2O$ was investigated by B. Lorenz *et al.* [8]. They performed ac susceptibility measurements for pressures up

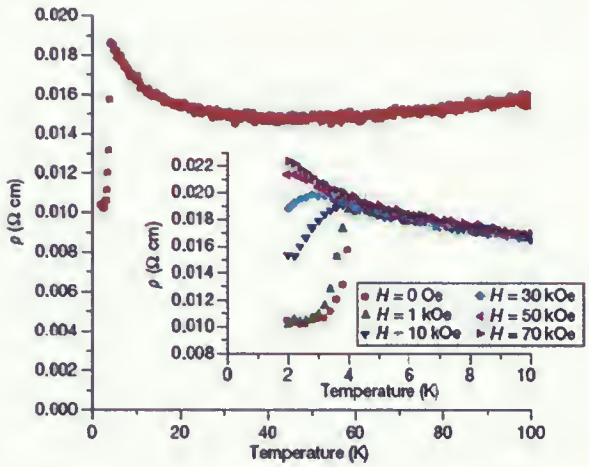

Figure 1.6: Resistivity (ρ) of $Na_xCoO_2 \cdot yH_2O$ under zero magnetic field. The inset figure shows the resistivity measured under various magnetic fields [7].

to 1.6 GPa and showed that the pressure coefficient of the T_c is negative and its pressure dependence is nonlinear as it is shown in Fig. 1.7. The magnitude of the average $d\ln T_c/dp \simeq$ -.07 GPa^{-1} is comparable to the pressure coefficient of electron-doped high T_c copper oxide superconductors with similar values of T_c . This might provide support to the assumption of two-dimensional superconductivity in $Na_{0.35}CoO_2 \cdot yH_2O$, which is similar to the cuprate systems, and suggests that intercalation of larger molecules may lead to an enhancement of T_c.

The properties of Na_xCoO_2 have attracted considerable attention from various research groups. It is hoped that study of Na_xCoO_2, especially $Na_{0.7}CoO_2$ (the host component of superconducting material) systems may shed new light in the nature of superconductivity in high T_c. Several different methods have been used to fabricate and characterize this compound.

T. Motohashi [6] *et al.* facilitated a new synthesis method called "The rapid heat-up" technique. This enabled them to control the concentration of Na precisely by avoiding *Na*

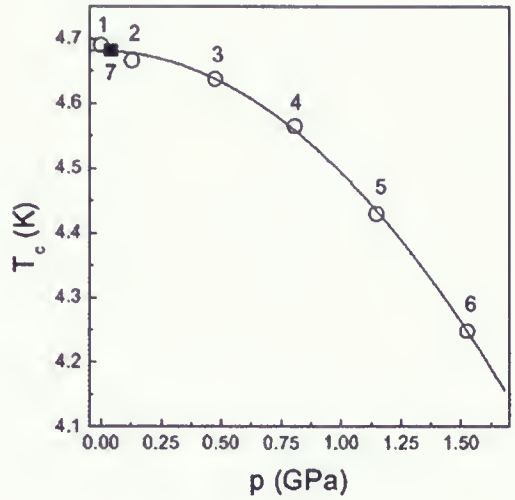

Figure 1.7: Pressure dependence of T_c of $Na_{0.35}CoO_2{\cdot}yH_2O$. The open circles are data taken at increasing pressure, the filled square indicates T_c after the pressure was completely released [8].

evaporation during sample firing. They showed that the maximum weight loss of Na will occur in the range of $500 - 750°C$ and it is $\approx 7.5\%$ Fig. 1.8. This value is too large so it can not be explained only with decarbonation of the raw materials ($\approx 5.7\%$). This suggests that there exists simultaneous Na evaporation in this temperature region. Further investigation on the sample preparation procedure has revealed that at temperatures as low as $500°C$ a chemical reaction between Na_2CO_3 and Co_3O_4 is not active but Na evaporates.

The phase diagram of non-hydrated Na_xCoO_2 has been reported By M.L.Foo [9] *et al.*. Concentration was changed by using a series of chemical reactions. Fig. 1.10 shows that as x increases from 0.3, the ground state goes from a paramagnetic to a charge order insulator (at x = 0.5) to a Curie-Weiss metal (around 0.7), and finally to a weak-moment magnetically ordered state (x > 0.75). Also it was shown [9] that resistivity will increase by increasing the concentration of sodium Fig. 1.11

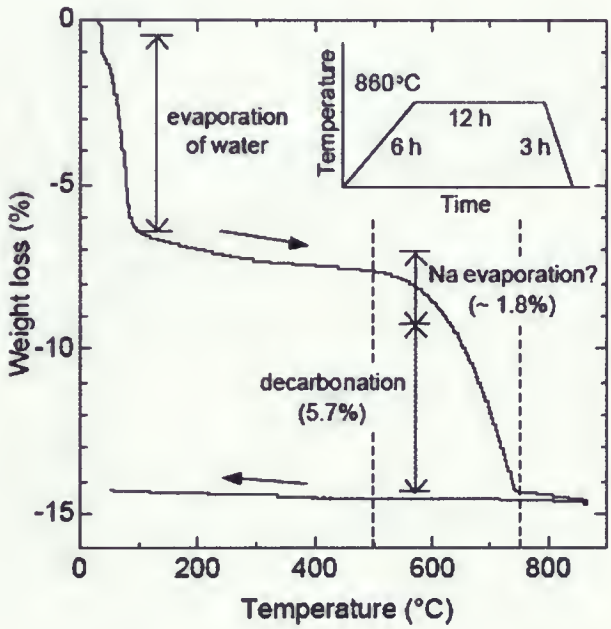

Figure 1.8: Thermogravimetric curve for the phase-information process of $Na_{0.55}CoO_{2+\delta}$ in flowing O_2 gas [6].

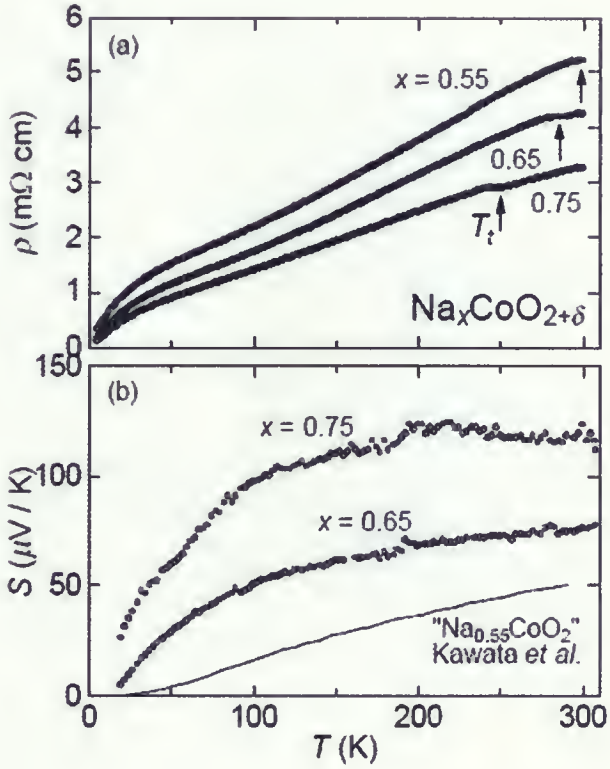

Figure 1.9: Temperature dependence of ρ and S of Na_xCoO_2 [6].

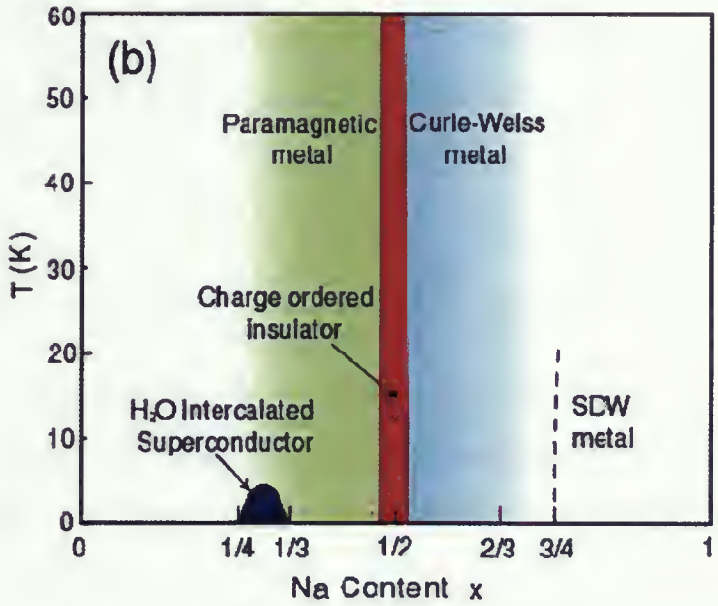

Figure 1.10: Phase diagram of non-hydrated Na_xCoO_2 [9].

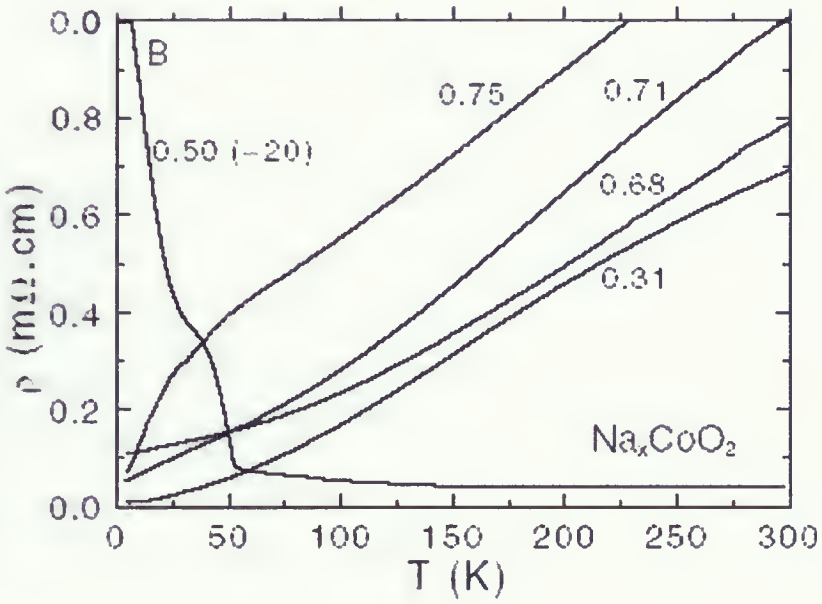

Figure 1.11: In plane resistivity of single crystal of Na_xCoO_2 [9].

D.Prabhakaran [10] *et al.* made Na_xCoO_2, with $x = 0.5, 0.6, ..., 0.95$. and reported that the residual Co_3O_4 impurities were above the detectable limit in samples with lower concentration of Na, i.e. x $<$ 0.65. Investigation of Na_xCoO_2 single crystals showed:

1. Transitions at 320 K, 270 K and 22 K present for all Na doping levels investigated.

2. A strong increase in magnetization below 8 K.

Iliev *et al.* [11] used polarized Raman spectra to study single crystal Na_xCoO_2 (x $\simeq$ 0.71) and found out that the spectra differ significantly between ab and ac surfaces. This provides evidence that within hours after preparation, the ac surface, unlike the ab one, is strongly disordered. In several days the disorder extends over the ab surface.

Sugiyama [12] have investigated magnetic properties of layer cobaltites for single crystal Na_xCoO_2 (x= 0.6 and x= 0.9) by positive muon spin rotation and relaxation spectroscopy together with magnetic susceptibility and specific heat measurements. Zero field μ^+SR

measurement indicates a transition from a paramagnetic to an incommensurate spin density wave state at 19 K(=T_{SDW}). They showed $Na_{0.6}CoO_2$ is paramagnetic down to 1.8 K , so the magnitude of T_{SDW} strongly depends on x. It was explained by a Hubbard model within a mean field approximation on a two dimensional triangular lattice in the CoO_2 plane. By considering the magnitude of the electronic specific heat parameter of $Na_{0.6}CoO_2$ they understood that Na_xCoO_2 is unlikely to be a typical strongly correlated electron system.

Mukhamedshin *et al.* [13] have compared ^{23}Na NMR and magnetic susceptibility of powders of samples of Na_xCoO_2 where $0.5 \leq x \leq 0.7$. The NMR spectra were found to be identical for all samples , which indicates that the dominant phase has a single composition $x \approx 0.7$. Their local susceptibility of the magnetic cobalt sites displays a large enhancement below 100K with respect to the usual high T Curie-Wiess law. A very distinct and much weaker Pauli like magnetism is detected for $x \approx 0.35$, which is the parent of the superconducting hydrated compound.

Transmission-electron-microscopy [14] reveals the presence of a superstructure in Na_xCoO_2 for x ranging from 0.75 to 1. The appearance of this superstructure can be fundamentally understood by Na-ion ordering occurring at low temperatures. Measurement of the electric transport properties reveal evident anomalies in the resistivity curve in association with the Na ordering. Antiferromagnetism appears for the samples $0.75 \leq x \leq 1$. In particular Na_xCoO_2 shows a sharp antiferromagnetic transition at the temperature of T_N=4 K.

The Hall coefficient R_H of Na_xCoO_2 (x=0.65) behaves anomalously at high temperature [2]. From 200 K to 500 K, R_H increases linearly with T up to 8 times the expected Drude value, with no sign of saturation. Behavior of R_H together with the thermopower Q provides strong correlation evidence. The dielectric function of single crystal Na_xCoO_2 (x = 0.82) was measured, using spectral ellipsometry [15]. The results show bulk antiferromagnetism at T_N=19.8 K and two other prominent transitions as a function of temperature. The first transition at T = 280 K involves marked changes of the electronic and the lattice

response, that are indicative of charge ordering in the CoO_2 layers. The second transition coincides with T_N=19.8 K and reveals a sizeable spin charge coupling. The results are discussed in terms of charge ordering and formation of magneto-polarons due to a charge-induced spin-state transition of adjacent Co^{+3} ions. Takeuchi *et al.* [16] have investigated the magnetic properties of Na_xCoO_2 (x = 0.75) from 2 K to 300 K. The temperature dependence of the magnetic susceptibility shows Curie-Wiess behavior down to 15 K. Spin glass like characteristics, the cusp anomaly seen at 3 K, irreversibility between zero-field and field cooled magnetic susceptibility below 13 K are observed. Results showed that samples were not conventional itinerant paramagnets.

In this thesis, electrical and magnetic properties of Na_xCoO_2 and $Na_xCoO_2{\cdot}yH_2O$ were studied. Samples of Na_xCoO_2 with x=0.25, 0.4, 0.5, 0.6, 0.7, 0.75 were synthesized using the solid state reaction method in two batches. Samples of the first batch were annealed in O_2, while the second batch were annealed in Argon. Resistivity measurements on the Argon annealed samples show that they were all insulators whereas samples annealed in O_2 exhibited metallic behavior. X-ray powder diffraction data, for all concentrations of x have shown a mixed phase, containing Co_3O_4 and Na_xCoO_2 with x$\simeq$ 0.71. The amount of Co_3O_4 present was calculated by using Fullprof software.

Magnetization and resistivity measurements of polycrystalline Na_xCoO_2 annealed in O_2 were performed. It has revealed a number of features present over a range of Na doping. Magnetization showed a clear peak at 35 K which is due to the Co_3O_4 impurity. Magnetoresistance measurements on $Na_{0.71}CoO_2$ showed two transitions, $T1._1$= 20 K (magnetic transition) and T_2=280 K (structural transition) and neither of them were dependent on the strength of the magnetic field. Hydrostatic pressure dependent-resistivity measurements on Na_xCoO_2 were performed for pressure ranges from atmosphere to 11 kbar. Resistivity decreased with increasing pressure. Temperature dependence of magnetization was studied for $Na_xCoO_2{\cdot}yH_2O$, which showed superconducting behavior. Also, magnetic field dependence

of magnetization was measured at different temperatures. The organization of this thesis is as follow. In chapter 2, the preparation method for Na_xCoO_2, $Na_xCoO_2 \cdot yH_2O$ and XRD results for Na_xCoO_2 will be discussed. Chapter 3 will be talk about Magnetization measurement of Na_xCoO_2 and $Na_xCoO_2 \cdot yH_2O$. Chapter 4 will give the information of experimental setup for electrical measurements, resistivity changes under pressure and magnetoresistance measurement of Na_xCoO_2 and finally conclusion in chapter 6.

Chapter 2

Method of preparation

2.1 Preparation of the ceramic samples of Na_xCoO_2

Ceramic samples of Na_xCoO_2 ($x = 0.25, 0.4, 0.5, 0.6, 0.7, 0.75$) were prepared by using a standard Solid state reaction method. [1] Samples were synthesized by mixing stochiometric amounts of high purity Na_2CO_3 (99.98% Alfa asear) and Co_3O_4(99.98% Alfa asear) powders by using mortar and pestle. This mixture was then sintered at $750 - 850°C$ for 12 hours in flowing O_2. The furnace was calibrated using a standard thermocouple. The sintered powders were then pressed into pellets by applying a force of approximately 10 tones using a stainless steel dye of 13 mm. diameter. Pellets of approximately 1-4 mm. diamater, were sintered again in $750 - 850°C$ for another 12 hours. Prabhakaran *et al.* [10] showed that products formed more rapidly if mixed powders were used for sintering rather than pressed pellets in the first sintering period. The heating method used was so called "The Rapid heat" method [6]. In this technique, a powder mixture of Na_2CO_3 and Co_3O_4 of an appropriate ratio is directly placed in the furnace which is preheated at $750 - 850°C$, in order to trigger instantaneous chemical reaction between the raw materials (see chapter 1).

[1] The solid state reaction method is normally used to synthesize inorganic compounds such as oxide. In this method, ingredients are weighed, mixed in a mortar with a pestle, and then heated in an electric furnace. Substances usually become liquid when they are heated; the driving force of the solid reaction is diffusion of atoms (ions) between solid substances. Therefore, the reaction happens at a temperature less than the melting points of each substance. [17]

A similar procedure was used for synthesizing another set of samples with the above mentioned concentrations. The only difference in the reaction method was that these samples were sintered in flowing Argon instead of O_2. Those samples that were sintered under flowing Argon, and they all show an insulting behavior in resistivity measurements. Some of those were annealed once again in flowing O_2.

2.2 Preparation of $Na_xCoO_2 \cdot yH_2O$

$Na_xCoO_2 \cdot yH_2O$ was prepared by chemically de-intercalating $Na_{0.7}CoO_2$ with bromine as an oxidizing agent as it was reported in the literature [18, 4, 9, 19]. One half gram of $Na_{0.7}CoO_2$ was stirred in 20mL of a 6 molar Br_2 solution in acetonitrile at room temperature for 5 days. Schaak *et al.* [18] used different stochiometric amounts (0.5X, 1X, 10X, 20X, 100X, ..) of Br_2 ("1X" indicates that the amount of Br_2 used is exactly the amount that would theoretically be needed to remove all of the sodium from $Na_{0.7}CoO_2$). They found that the fully hydrated single phase $Na_xCoO_2 \cdot yH_2O$ occurs for higher Br_2 concentrations. The product was washed in acetonitrile and then with distilled water a few more times. The fully hydrated $Na_xCoO_2 \cdot yH_2O$ was prepared by placing 0.5g of $Na_{0.3}CoO_2$ in an open 20mL vial, which was then sealed inside the larger screw-cap jar that was loaded with 10 mL of H_2O. Evaporation of the water inside the sealed container creates a humidified chamber in which the samples are hydrated over a period of 1-2 days. Scientists are attempting to generate a new method for fabricating $Na_{0.3}CoO_2 \cdot (4/3)H_2O$ to avoid the associated environmental hazards which are due to manipulating large amounts of high concentrations of Br_2. Chou *et al.* [20] used an electrochemical route for the de-intercalation step which allows a better control of the Na content. Park *et al.* [21], synthesized $Na_xCoO_2 \cdot yH_2O$ by stirring $Na_{0.7}CoO_2$ in $Na_2S_2O_8$.

2.3 X-ray diffraction

To characterize the samples and ascertain their quality, X-ray powder diffraction was performed on all the samples at the Max-Planck Institute in Stuttgart, Germany. The wavelength of the (Cu K_α line) incident beam used was 1.54 $A°$. The range of 2θ was 5.01° to 89.99°. Results show the residual Co_3O_4 impurities above the detectable limit remained for samples with $x < 0.65$, and conditions to eliminate this have yet to be identified. X-ray results for all samples with different concentrations reveal similar peaks which indicate that they are in stable phase. A search in the database suggested that the best structural match is $Na_{0.7}CoO_2$. A stable phase was observed even for those samples whose Na over Co ratio was less than 0.70. Previous results in the literature reported excess Co_3O_4 in the final product for these reagent ratios. XRD patterns show a weak presence of Co_3O_4, but this presence was also detected in magnetization measurements as a clear peak at $T \simeq 35$ K which is due to the antiferromagnetic ordering transition of Co_3O_4 [10]. A thin layer of glassy material was formed on the sample $Na_{0.7}CoO_2$ due to the rapid heat-up method. After removing clear glassy materials from sample's surface, X-ray measurement showed a perfect ceramic of $Na_{0.7}CoO_2$. To check the results on the structural properties of the samples, all x-ray data were compared with structure of $Na_{0.7}CoO_2$ and Co_3O_4. Previous measurements [22, 23, 24] have revealed the structure of $Na_{0.7}CoO_2$ consists of layers of edge sharing CoO_6 octahedra, where the cobalt atoms form a triangular lattice. For the hexagonal unit cell, the lattice constant a_H=2.84 $A°$ and c_H=11.01 $A°$ and space group is $P6_3/mmc$ [25], and is shown in Fig. 2.1. Figures 2.2, 2.3, 2.4, 2.5, show X-ray data of Na_xCoO_2. They were analyzed by using Fullprof. The Fullprof [2]program has been mainly developed for Rietveld analysis (structure profile refinement) of neutron (constant wavelength, time of flight, nuclear and magnetic scattering) or X-ray powder diffraction data collected at constant or variable step

[2][26]

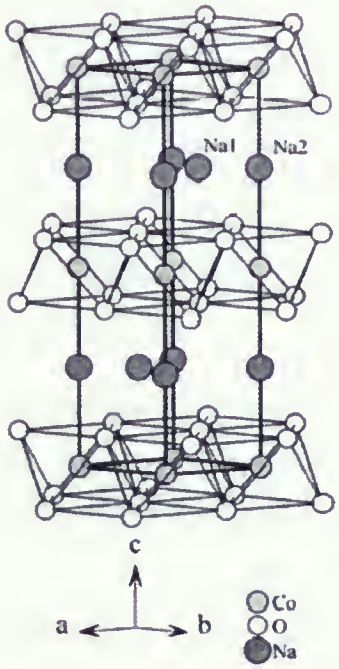

Figure 2.1: Crystal structure of $Na_{0.7}CoO_2$, space group $P6_3/mmc$. Co atoms are octahedrally coordinated to six oxygen atoms. The CoO_6 octahedra share edges to form layers. Na ions are in two partially occupied sites, Na1 and Na2. The figure is reproduced from Jorgensen's paper [24]

in scattering angle 2θ. The program can be also used as a Profile Matching (or pattern decomposition) tool, without the knowledge of the structure. Single crystal refinement can also be performed alone or in combination with powder data. Time of flight (TOF) neutron data analysis is also available. Energy dispersive X-ray data can also be treated but only for profile matching. Fullprof_2k has been developed from the standard Fortran77 [27]. In order to determine the origin of impurity peaks in the x-ray data, the Co_3O_4 structure was used in refinement and the results showed that most of the impurities belong to it. Co_3O_4 has a cubic structure with lattice parameter a_c=8.0821 $A°$ and space group Fd3m. Calculation show samples of Na_xCoO_2 where x$\neq$ 0.7 are consist of about 15 percent Co_3O_4 [25]. Information about the samples and their probable impurities were summerized at Table 2.1.

Table 2.1: Different concentration of sodium

Sample name	**Preparation condition**	**Probable impurities**
$Na_{0.25}CoO_2$	flowing O_2	$Na_{0.70}CoO_2$, Co_3O_4 and NaOH
	flowing Argon	$Na_{0.70}CoO_2$, Co_3O_4 and CoO
$Na_{0.3}CoO_2$	flowing O_2	$Na_{0.70}CoO_2$, Co_3O_4 and NaOH
$Na_{0.5}CoO_2$	flowing O_2	$Na_{0.70}CoO_2$, Co_3O_4
	flowing Argon	$Na_{0.70}CoO_2$, Co_3O_4 and *CoO*
	flowing Argon then O_2	$Na_{0.70}CoO_2$, Co_3O_4 and *NaOH*
$Na_{0.7}CoO_2$	flowing O_2	No impurity
	flowing Argon	$Na_{0.70}CoO_2$, Na_2CO_3 and Co_3O_4
	flowing Argon then O_2	$a_{0.70}CoO_2$ and Co_3O_4

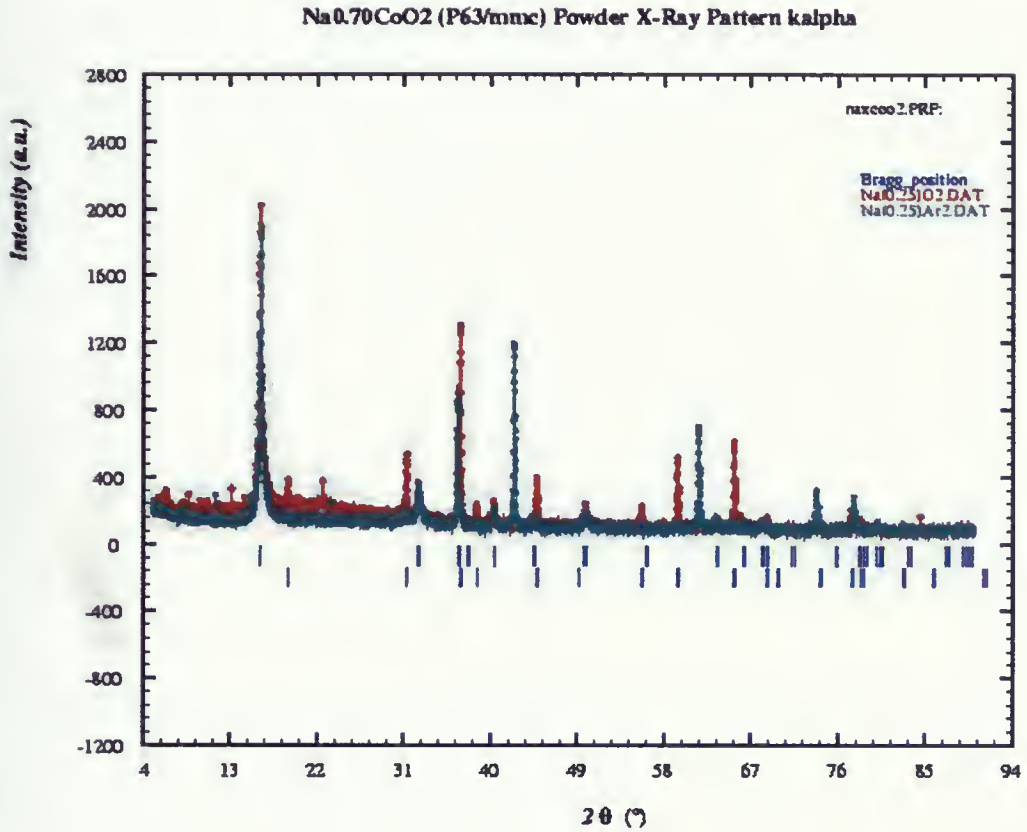

Figure 2.2: Sample $Na_{0.25}CoO_2$ reacted in flowing O_2 (red circles), Sample $Na_{0.25}CoO_2$ reacted in flowing Argon (green circles)

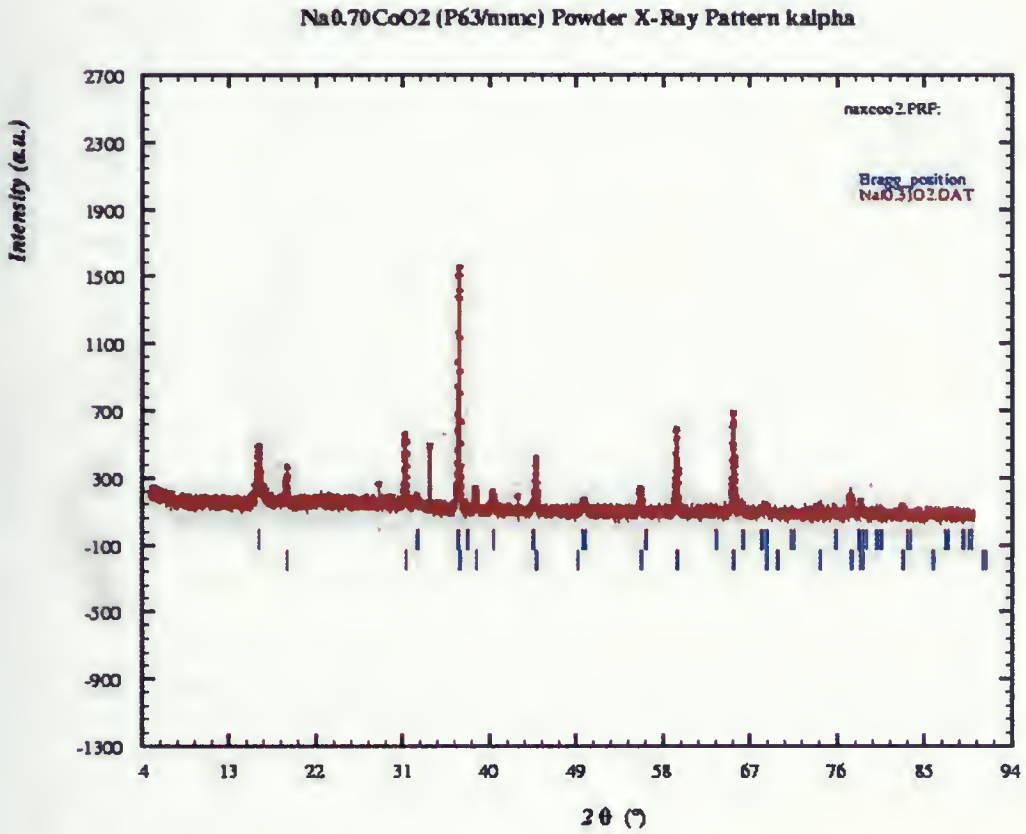

Figure 2.3: Sample $Na_{0.30}CoO_2$ reacted in flowing O_2 (red circles)

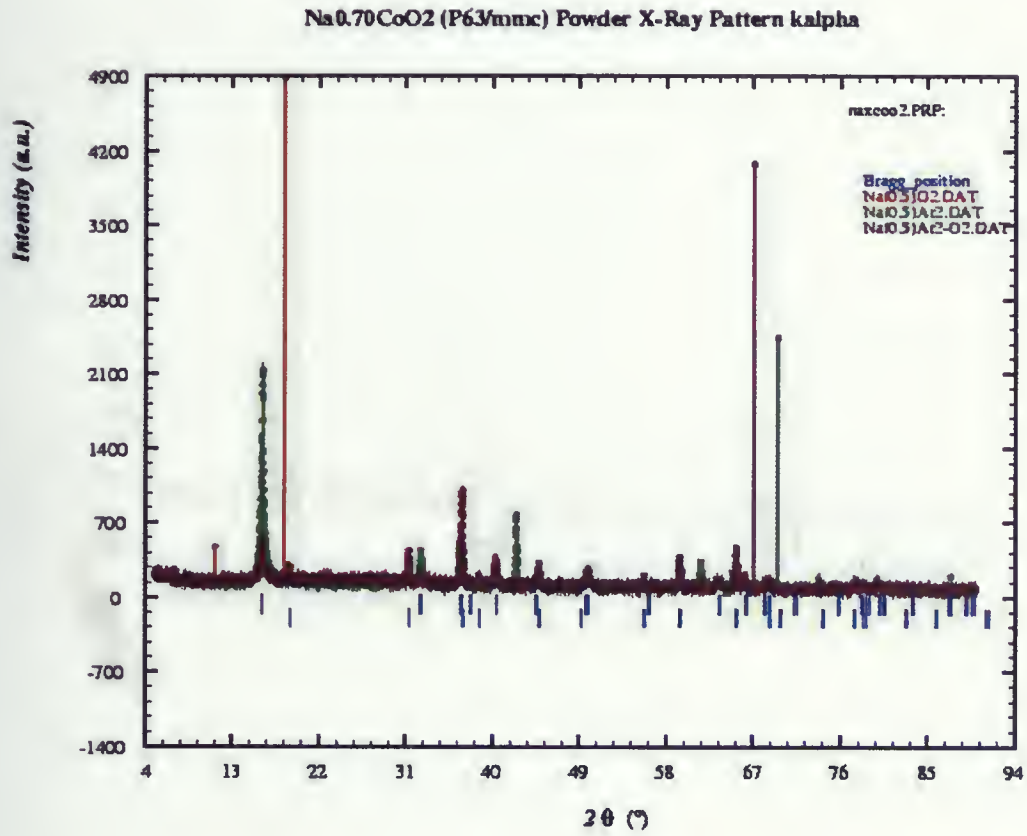

Figure 2.4: Sample $Na_{0.50}CoO_2$ reacted in flowing O_2 (red circles), Sample $Na_{0.50}CoO_2$ reacted in flowing Argon (green circles), Sample $Na_{0.50}CoO_2$ reacted in flowing Argon then O_2 (dark red circles)

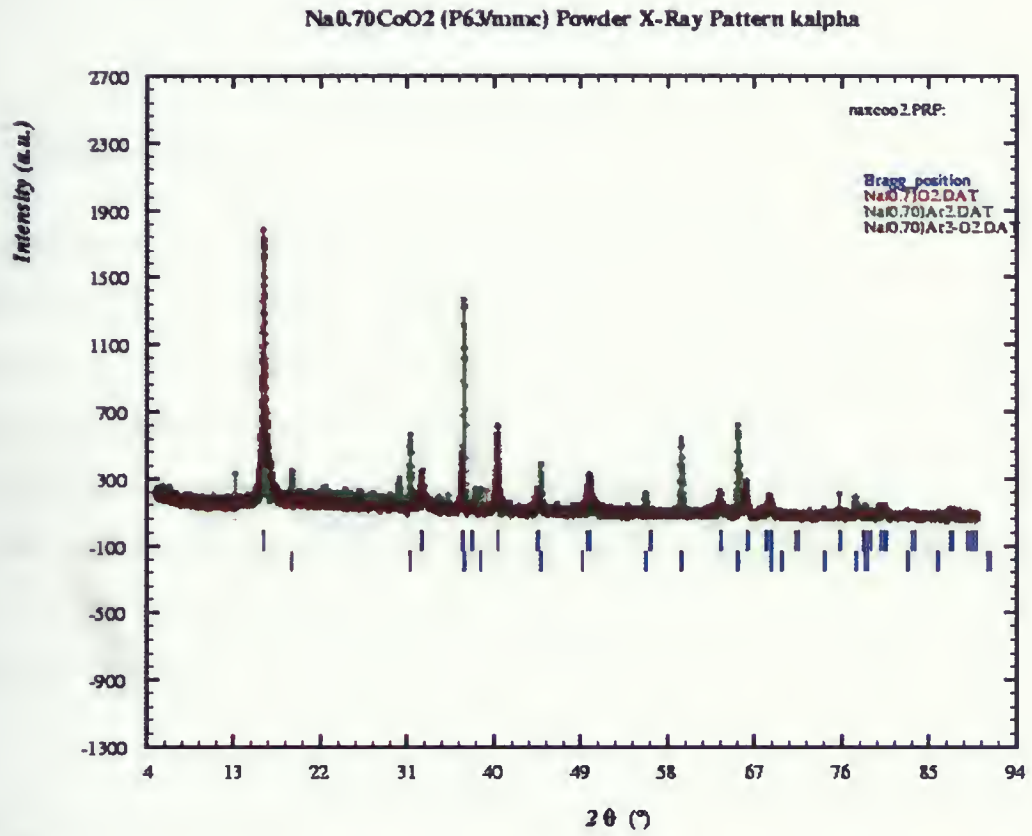

Figure 2.5: Sample $Na_{0.70}CoO_2$ (red circles), Sample $Na_{0.70}CoO_2$ reacted in flowing Argon(green circles), Sample $Na_{0.75}CoO_2$ reacted in flowing Argon then O_2 (dark red circles)

Chapter 3

Magnetization

3.1 Magnetism

When a material is placed in a magnetic field, the magnetic forces of the material's electrons will be affected. However, materials can react differently in the presence of an external magnetic field. This reaction is dependent on a number of factors such as the atomic and molecular structure of the material, and the net magnetic field associated with the atoms. This magnetic field may have three origins which are the electron orbital motion, the change in orbital motion caused by an external magnetic field and the spin of the electrons. The response of the material to the magnetic field is called magnetization (M) and for most material it is proportional to H by Eq. 3.1 :

$$M = \chi H \tag{3.1}$$

The proportionality constant, χ, is the magnetic susceptibility. Fig 3.1 shows the range at which the magnetic moment changes for different kinds of magnetic materials [28]. The four common types of magnetism are:

1. Diamagnetism
2. Paramagnetism
3. Ferromagnetism
4. Antiferromagnetism

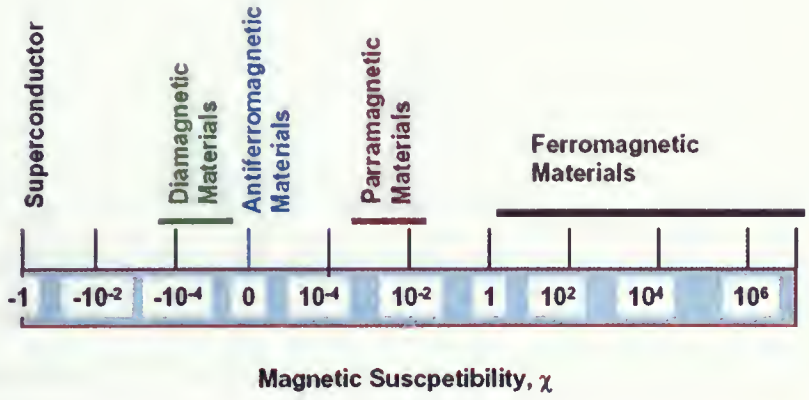

Figure 3.1: Magnetic susceptibility (χ)

3.1.1 Diamagnetism

Diamagnetism is a very weak form of magnetism that is only exhibited in the presence of an external magnetic field. The orbital motion of electrons creates tiny atomic current loops, which produce magnetic fields. When an external magnetic field is applied to a material, these current loops will tend to align in such a way as to oppose the applied field (atomic version of Lenz's law). Induced magnetic fields tend to oppose the change which created them. The induced magnetic moment is very small and the direction is opposite in the direction to applied field. Typically, $\chi = -1 * 10^{-6}$emu/mol [29, 30].

3.1.2 Paramagnetism

Paramagnetism refers to the material having a small and positive susceptibility to magnetic fields. These materials are slightly attracted by a magnetic field and the material dose not hold the magnetic properties when the external field is removed. Paramagnetic properties are due to the presence of some unpaired electrons and from the realignment of the electron orbits caused by the external magnetic field. Paramagnetic materials exhibit magnetization

according to **Curie-Weiss's Law**:

$$\chi_p = C/(T - T_C) \tag{3.2}$$

In the equation 3.2, C is a material-specific curie constant and T is temperature in Kelvin, T_c is a Weiss constant (Curie temperature) and it is indicative of intermolecular interactions among the moment.

If $T>T_C$, paramagnetic interaction exist

If $T<T_C$, ferromagnetic interaction where $T_C > 0$ and antiferromagnetic behavior where $T_C < 0$ [28, 30].

3.1.3 Ferromagnetism

Ferromagnetic materials have a large and positive susceptibility to an external magnetic field. They exhibit a strong attraction to magnetic fields and are able to keep their magnetic properties after the external field has been removed. Ferromagnetic materials have some unpaired electrons so their atoms have a net magnetic moment. They get their strong magnetic properties due to the presence of magnetic domains. In these domains, large numbers of atom moments (10^{12} to 10^{15}) are aligned parallel so that the magnetic force within the domains is strong. When a ferromagnetic material is in unmagnetized state, the domains are nearly randomly organized and the net magnetic field for the part as a whole is zero. When a magnetizing force is applied, the domains become aligned to produce a strong magnetic field within the parts. Ferromagnetic material has a phase transition that occurs at the critical temperature, T_C which is Curie temperature and above T_C paramagnetism exists [28, 30, 31].

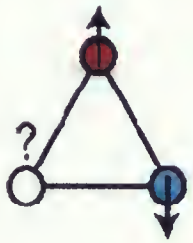

Figure 3.2: Spins in a triangular lattice

3.1.4 Antiferromagnetism

In Antiferromagnetism, the spins of magnetic electrons align in a regular pattern with neighboring spins in opposite directions. Generally, antiferromagnetism occurs at a low temperature and become disordered above a certain temperature. This temperature is called **Neel temperature** and above this temperature, the material is typically paramagnetic. The magnetic susceptibility of an antiferromagnetic material appears to go through a maximum as the temperature is lowered [28, 30, 31].

3.2 Magnetization of Na_xCoO_2

Na ions are sandwiched between triangular lattice of CoO_2 layers in Na_xCoO_2 (see Fig. 1.3). On triangular lattices "Geometrical frustration" is an important factor that shape the behavior of electrons. In an insulating lattice, the coulomb repulsion force is relieved if each electron can point its spin antiparallel to their nearest neighbors. This arrangement of spins leads to a **Neel** state in which spins alternate up and down along each bond direction. However, geometric frustration prevent such ideal regularity on the triangular lattice. As is shown in Fig.3.2 two of the three electrons must share the same spin orientation [32]. At absolute zero, the spins remain in a disordered quantum state with no certain pattern which

is often called "spin liquid". Understanding the spin liquid state is the major goal of the science of the strongly correlated materials. Initial results [1] obtained on Na_xCoO_2 with x close to (2/3), showed that the material is an excellent electrical conductor. In a metal, the percentage of electron spins which can be field-aligned is very small, and shrink to zero by decreasing temperature. By contrast, in Na_xCoO_2, the amount of susceptible spin equals the charge carrier population (holes), and stays unchanged with decrease in temperature [33, 2]. For metallic system such as Na_xCoO_2, the total susceptibility χ(T) is given by Eq.3.3

$$\chi(T) = \chi_s + \chi_{dia} + \chi_{VV} + \chi_d(T) \tag{3.3}$$

Where χ_s represents the Pauli paramagnetic component from s electrons. As some of the s electrons can be thought to be localized on the oxygen atoms and hence would not contribute to the electrical and magnetic properties. However, there is no knowledge about the nature of s electrons from sodium ion [33]. In comparison to the total susceptibility χ(T) at 300 K ($\simeq 800 * 10^{-6}$emu/mole), the diamagnetic term χ_{dia}, to which the ion cores contribute, is a small correction. The term χ_{VV} has the origin in the temperature-independent orbital paramagnetic susceptibility in insulators. In a compound containing Co ions, this generally has a large contribution. These three terms can be grouped together as χ_0. The temperature dependent spin paramagnetism $\chi_d(T)$ arises from the localized character of the d electrons. Therefore Eq. 3.3 can be expressed as Eq. 3.4:

$$\chi(T) = \chi_0 + C/(T - \theta) \tag{3.4}$$

Magnetization data can be parameterized by Eq. 3.4. Table 3.1 shows fitting parameters which are reported by other groups.

The triangular lattice becomes superconducting when water molecules intercalate to form a layer between the Na ions and CoO_2 layer. The superconducting phase exist just in the narrow interval $1/4 < x < 1/3$ [9] see Fig. 1.10. An important factor seems to be the ability

Table 3.1: Result of fitting magnetization data with Curie-Weiss equation

Author	**Sample name**	**Curie constant (C) emu K/mole**	**Curie Temperature (θ) K**	χ_0 **emu/mole**
Foo *et al.* [9]	$Na_{0.75}CoO_2$	2.81	-150	-
Motohashi *et al.* [34]	$Na_{0.75}CoO_2$	0.234	-166.4	-
Ray *et al.* [33]	$Na_{0.7}CoO_2$	0.276	-116	$1.6*10^{-4}$
Miyoshi *et al.* [35]	$Na_{0.75}CoO_2$	0.369	-139	$1.12*10^{-4}$
Ono *et al.* [36]	$Na_{0.67}CoO_2$	0.219	-285	$1.11*10^{-4}$
Sales *et al.* [37]	$Na_{0.75}CoO_2$	0.16-0.23	-120	$1.71*10^{-4}$
Tojo *et al.* [38]	$Na_{0.75}CoO_2$	0.126	-109.6	$1.3*10^{-4}$
Gavilano *et al.* [39]	$Na_{0.7}CoO_2$	0.15	-103	$1.25*10^{-4}$
Takeuchi *et al.* [16]	$Na_{0.75}CoO_2$	0.15	-130.4	$0.85*10^{-4}$
Chou *et al.* [40]	$Na_{0.75}CoO_2$	0.147	-125	$2*10^{-4}$

of water molecules to screen the strongly fluctuating electrostatic potential of the Na ions from the charge carriers in the CoO_2 layers.

3.3 Experimental procedure

3.3.1 SQUID

SQUID (Superconducting QUantum Interference Device) were invented in 1962 when B. D. Josephson [41] developed the Josephson junction. In the original form, SQUID consists of two Josephson tunneled junctions connected in parallel on a superconducting loop. Small applied current I flows through the junctions as a supercurrent, without developing a voltage, by means of cooper pairs tunneling through the barriers. However, when the applied current exceeds a certain critical value I_c, a voltage V is generated. The I_c, is an oscillator function of the magnetic flux ϕ, threading the loop with a period of one flux quantum ϕ_0 which is :

$$\phi_0 = 2 * \pi * \hbar/(2 * e) \simeq 2.0678 * 10^{-15} Tesla.m^2 \tag{3.5}$$

The oscillation arise from interference of the two waves describing the cooper pairs at the two junctions, in a way that is closely analogous to the interference between two coherent electromagnetic waves. Thus the SQUID is often called an interferometer. There are two main kinds of SQUIDs; DC and RF SQUIDS. The DC SQUIDs usually have two or more Josephson junctions. This makes them more sensitive but difficult and expensive to produce. The RF SQUIDs consist of a single junction interrupting a superconducting loop. It can be operated as a magnetometer by coupling it to the inductor of an LC-tank circuit excited at its resonant frequency by a RF current. The RF voltage across the tank circuit oscillates as a function of the magnetic flux in the loop, again with a period ϕ [42] Fig. 3.3 shows the structure of an RF-SQUID.

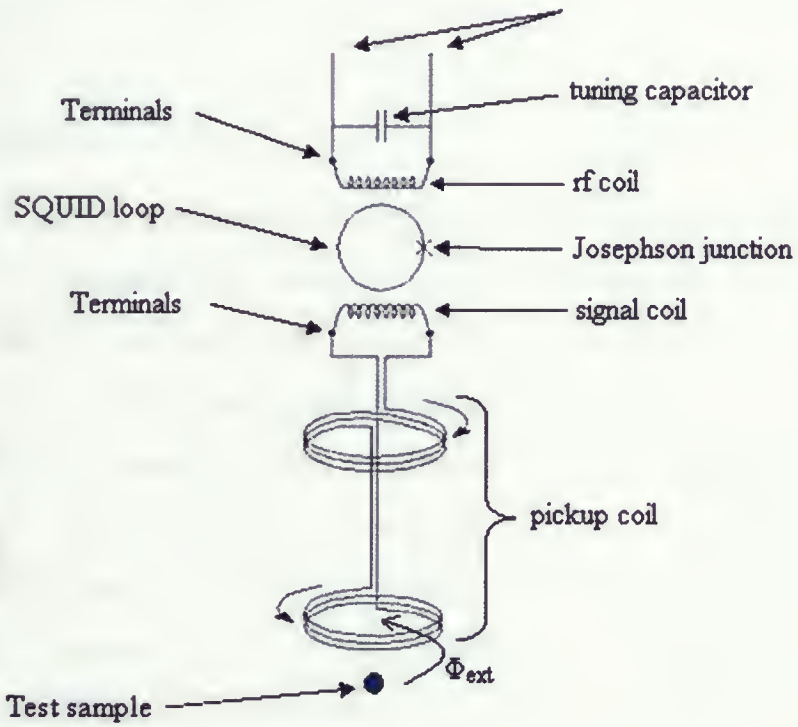

Figure 3.3: The RF SQUID inductively coupled to a resonant tank circuit [43]

Most SQUIDs are fabricated from lead or pure niobium. The lead is usually in the form of an alloy with 10 percent gold or indium, because pure lead is unstable when its temperature is repeatedly changed. The base electrode of the SQUID is made of a very thin niobium layer, formed by deposition, and the tunnel barrier is oxidized onto this niobium surface. The top electrode is a layer of lead alloy deposited on top of the other two, forming a sandwich arrangement. Measurements usually can be done in two forms of DC and AC magnetometery.

DC Magnetometery

DC magnetic measurements determine the equilibrium value of the magnetization in a sample. The sample is magnetized by a constant magnetic field and the magnetic moment of the sample is measured, producing a DC magnetization curve M(H). The moment is measured by force, torque or induction techniques, the last being the most common in modern instruments. Inductive measurements are performed by moving the sample relative to a set of pickup coils, either by vibration or one shot extraction. In conventional inductive magnetometers, one measures the voltage induced by the moving magnetic moment of the sample in a set of copper pickup coils. A much more sensitive technique uses a set of superconducting pickup coils and a SQUID to measure the current induced in superconducting pickup coils, yielding high sensitivity that is independent of sample speed during extraction. Inductive magnetometers can also be used to perform AC magnetic measurements [44].

AC Magnetometery

In AC magnetic measurements, a small AC drive magnetic field is superimposed on the DC field, causing a time-dependent moment in the sample. The field of the time-dependent moment induces a current in the pickup coils, allowing measurement without sample motion. The detection circuitry is configured to detect only in a narrow frequency band, normally at

the fundamental frequency(that of the AC drive field) [44].

3.4 Magnetization of ceramic sample Na_xCoO_2

Magnetic properties of Na_xCoO_2 (x=0.4, 0.6, 0.7, 0.8, 0.9) were studied using DC magnetization.[1] All the magnetic measurements on powder samples were performed immediately after the final sintering process. The same samples were remeasured after a few months and changes were observed especially in magnetization, which changed few times compared to the first measurement. Fig. 3.4 shows magnetization of $Na_{0.7}CoO_2$ which was measured in April and November 2004 where 1000 G field was applied. There was not any detectable change in the appearance of the particles or Co_3O_4 impurities in the re-measured sample. Prabhakaran [10] and Iliev [11] *et al.* also noticed similar changes. The fact that the sample is losing its magnetic moment in time period, might be due to the decomposition of Co_3O_4 or absorption of water from air. Since the superconductor sample is $Na_{0.35}CoO_2 \cdot (4/3)H_2O$, low Na concentration and water absorption reveal diamagnetic behavior in this sample.

Fig. 3.5 shows the temperature dependence of the magnetic moment for different concentration of Na in Na_xCoO_2. The peaks at T=35 K for sample with concentration of Na=0.4 and 0.6 is due to the antiferromagnetic ordering transition of Co_3O_4 [4, 9, 10]. A systematic decrease in magnetization with increasing x can be observed, which can be understood in terms of an decreasing ratio of Co^{+4} ($s = 1/2$) to Co^{+3} ($S = 0$). Since a stable phase was observed for x=0.7, those samples whose Na over Co ratio was less than 0.7, Co_3O_4 could not react with Na_2CO_3 completely and stays in the samples as an impurity, thus the antiferromagnetic peak of Co_3O_4 is sharper. Between (250 K-320 K), no anomaly was observed in magnetization measurements, while a peak was detected in resistivity measurements (see

[1]SQUID was calibrated using a 6 cm scan for *Pt* sample. The calibration error due to applying high fields, is estimated to be less than 0.1 %, however, there is up to 30 % error for very low fields [45].

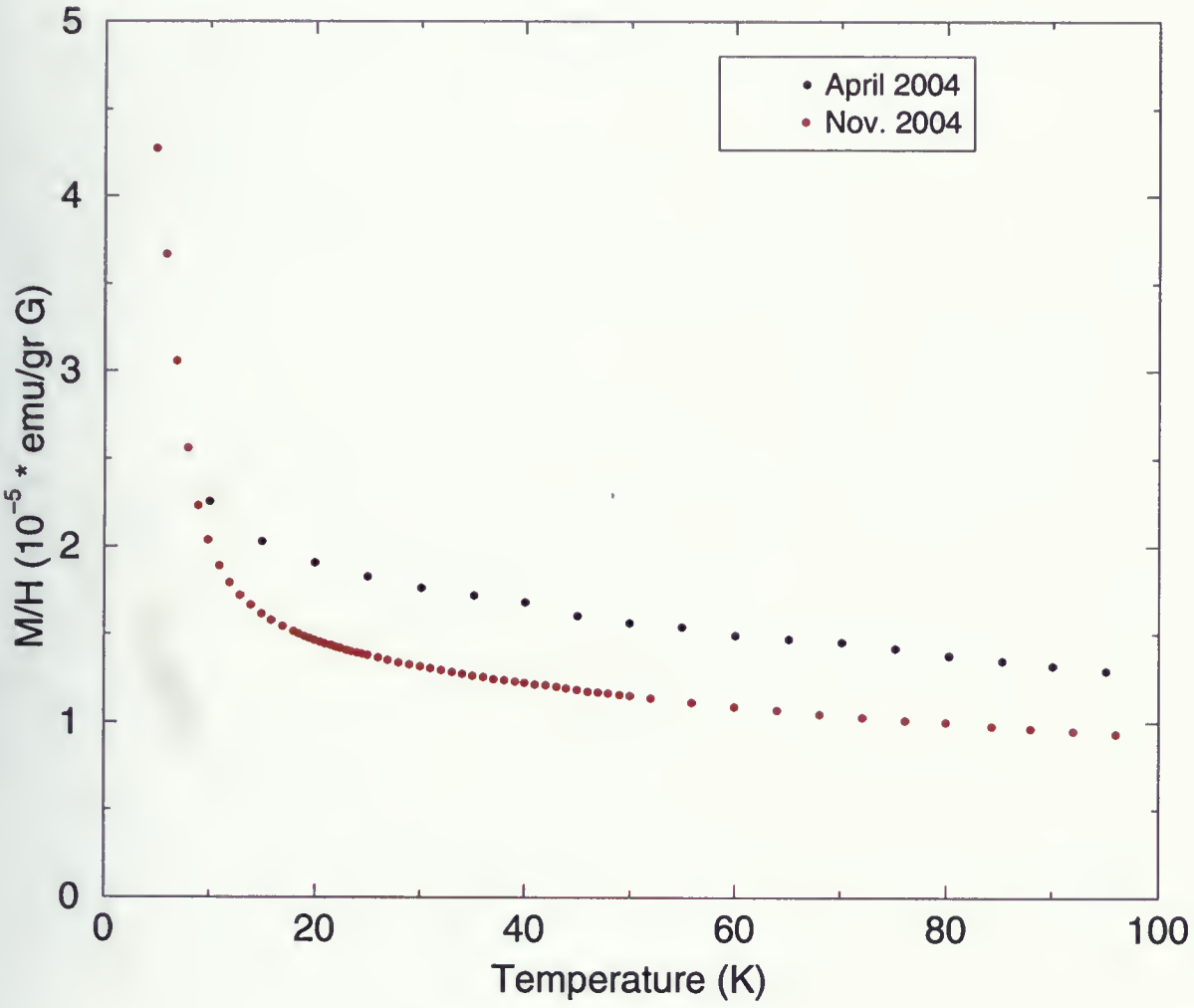

Figure 3.4: M/H measurement of sample $Na_{0.7}CoO_2$. Black circles were obtained on April 2004 and Red circles on November 2004. H=1000 G was applied.

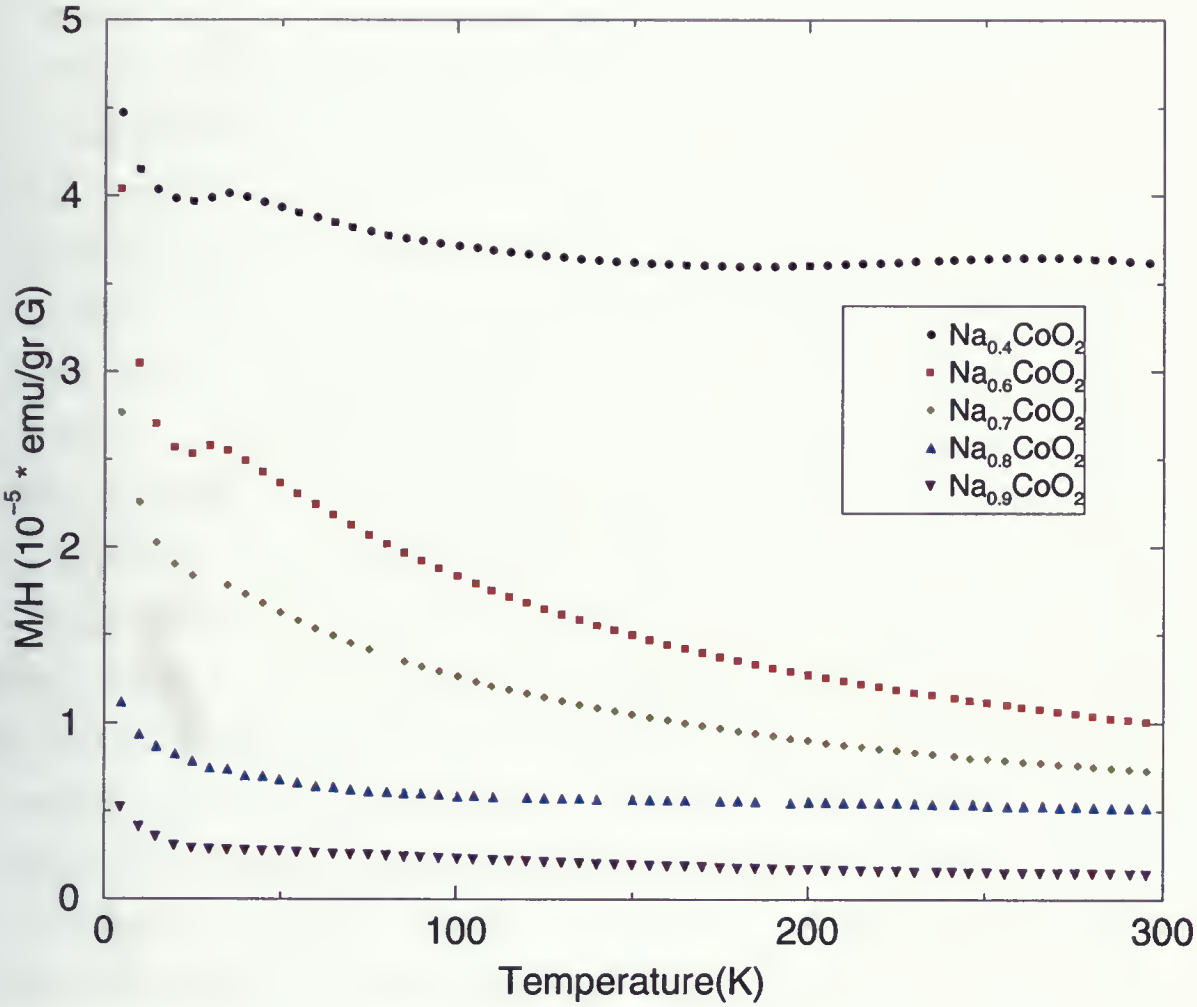

Figure 3.5: Magnetic susceptibility vs. Temperature of Na_xCoO_2 for different concentration of Na. Magnetic field of H=1000 G was applied

chapter 4). It is reported in single crystal samples that a notable peak was observed at around room temperature while they could not observed any peak in polycrystalline samples [10, 16]. Field Cool (FC) and Zero Field Cool (ZFC) measurements were performed on sample $Na_{0.7}CoO_2$. Since our interest was to see the magnetic transition T_m which was reported by different groups in the temperature ranges of 18 K-23 K [10, 34, 46], temperature dependent magnetization measurements were performed for different fields: H=25 G, 100 G, 1000 G, 10000 G between 5 K and 50 K. Fig. 3.6 and 3.7 show that there is a slight change between FC and ZFC when 25 G field was applied. This change is due to a weak magnetic interaction between domains and even a small field like 100 G can saturate domains as there is no difference between ZFC and FC for 100 G and higher fields. There are different opinions about the nature of this transition at T_m. Motohashi *et al.* [34] reported the existence of a magnetic transition at 22 K (=T_m) in polycrystalline $Na_{0.75}CoO_2$. From the observation of small changes in bulk susceptibility, while no transitions were found in $Na_{0.65}CoO_2$ down to 2 K. Positive muon spin rotation and relaxation (μ^+ SR) on the polycrystalline $Na_{0.75}CoO_2$ sample [46] indicated that the transition at 22 K is not induced by impurities but is an intrinsic change in the magnetism of the sample, although the sample was magnetically inhomogeneous. Also the μ^+SR result suggested that the ordered phase below T_m could be either a ferrimagnetic or a commensurate spin density wave state (SDW) while optical measurement showed that the origin of the transition is SDW [46, 47]. It was reported that there is a large difference in magnetic properties between single crystal and polycrystalline samples which is evident from T_m. Trying to fit magnetization data of sample $Na_{0.7}CoO_2$ with Eq. 3.4 in the temperature range of 50 K to 300 K, resulted in a Curie constant $C = 0.188 \pm 0.5 * 10^{-2}$ emu K/mol and urie temperature $\theta = -133 \pm 3.8$ K, $\chi_0 = 0.73*10^{-4} \pm 0.1*10^{-4}$ emu/mole and effective moment [2] is μ_{eff}=$1.22 \pm 0.25*10^{-2}$ μ_B/Co site if all the cobalt atoms are assumed equivalent. Fig. 3.8 illustrates the variation of the

[2][48]

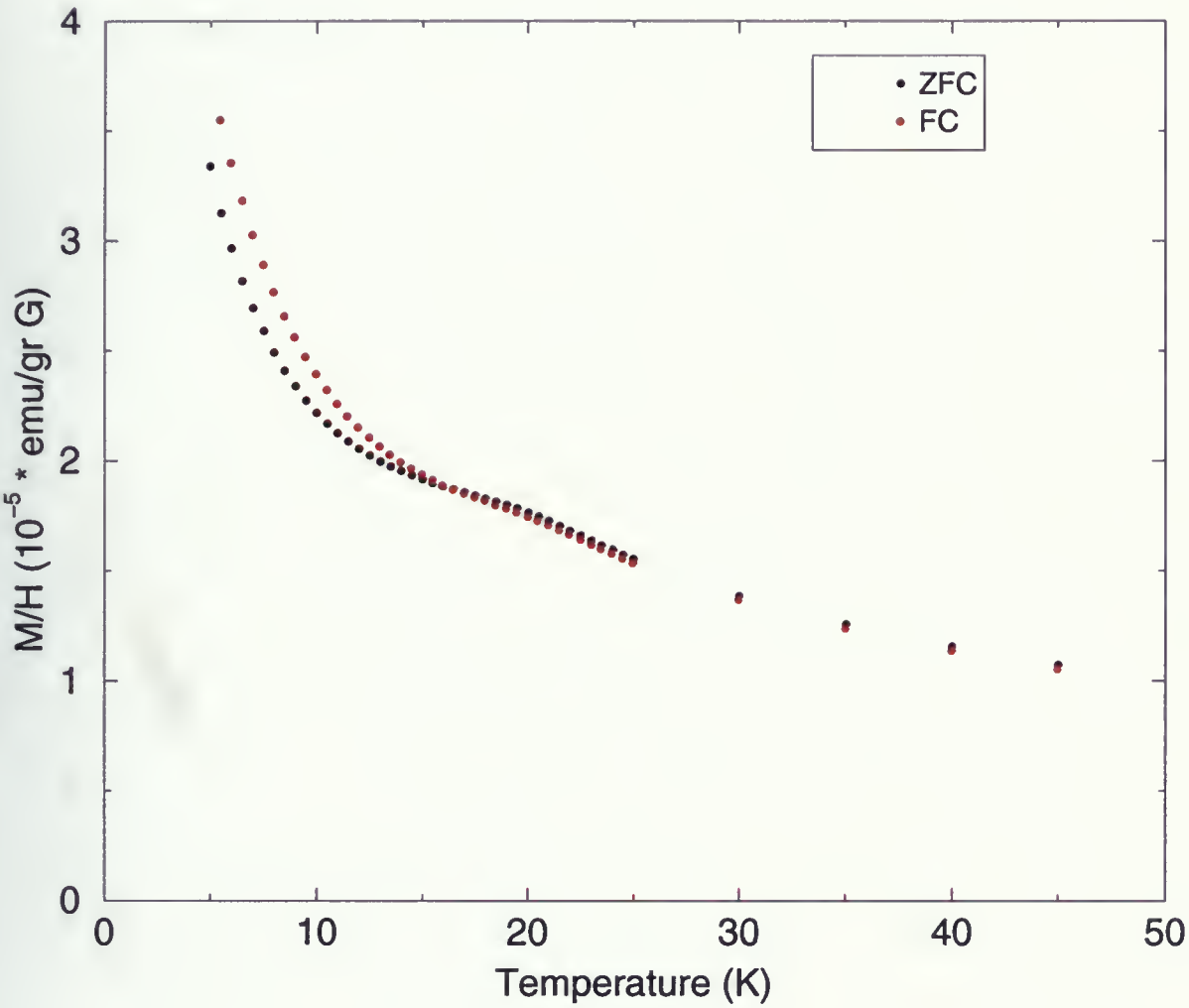

Figure 3.6: Magnetic susceptibility (χ) vs. Temperature for sample $Na_{0.7}CoO_2$. Black circles are ZFC and Red circles are FC. Magnetic field of H=25 G was applied.

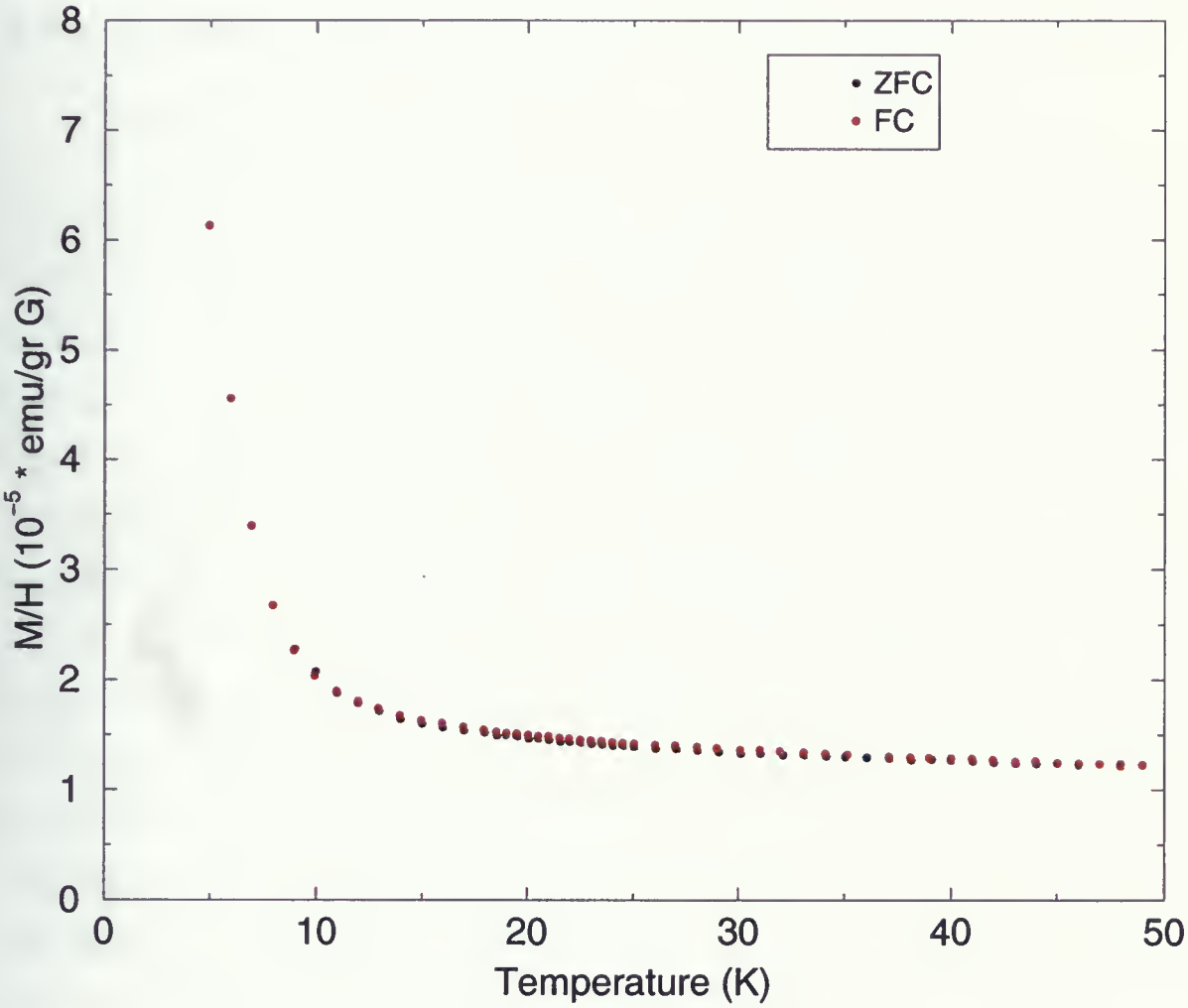

Figure 3.7: Magnetic susceptibility (χ) vs. Temperature for sample $Na_{0.7}CoO_2$. Black circles are ZFC and Red filled circles are FC. Magnetic field of H=100 G was applied.

ratio M(T)/H at temperatures between 5 K to 100 K for different fields of 100 G, 1000 G and 10000 G for sample $Na_{0.7}CoO_2$.[3]

3.5 Magnetization of Superconductor sample $Na_{0.35}CoO_2 \cdot (4/3)H_2O$

The discovery of superconductivity in $Na_{0.35}CoO_2 \cdot (4/3)H_2O$ generates interest to investigate the mechanism of superconductivity in this compound. Although the superconducting transition temperature, T_c is much lower than cuprate's, both systems have many common features. They both represent strongly correlated systems and it might be the reason that maximum critical temperature occurs just for a certain amount of H_2O and Na, and all the overdoped and underdoped materials have lower T_c. $Na_{0.35}CoO_2 \cdot (4/3)H_2O$ has two dimensional Co-O plane which is separated by Na and H_2O layers just as Cu-O layers alternate with rare earth dopant. Furthermore, both Co and Cu have spin 1/2. However, in contrast to square lattice form of cuprates, CoO_2 have a triangular form. To understand the pairing symmetry, experimental and theory studies have been performed on this sample and there are contradictions between results [49, 50, 51, 52]. It is still unclear whether superconductivity is originated from singlet or triplet pairing. Maska *et al.* [53] measured the upper critical field (H_{c2}) for the superconductor sample and showed that the unusual temperature dependence might be due to the field induced transition from singlet to triplet superconductivity. The nature of superconductivity in cobaltate remains an open issue. Magnetic properties seem to be a primary importance in these studies. Here, magnetization measurements were performed in low fields in order to find the values of lower critical fields. The superconduct-

[3]The difference between 10000 G and two other curves is probably due to the remnant fields from the shields surrounding the SQUID sensor which make the actual field at the sample differ by a few Gauss from the nominal filed.

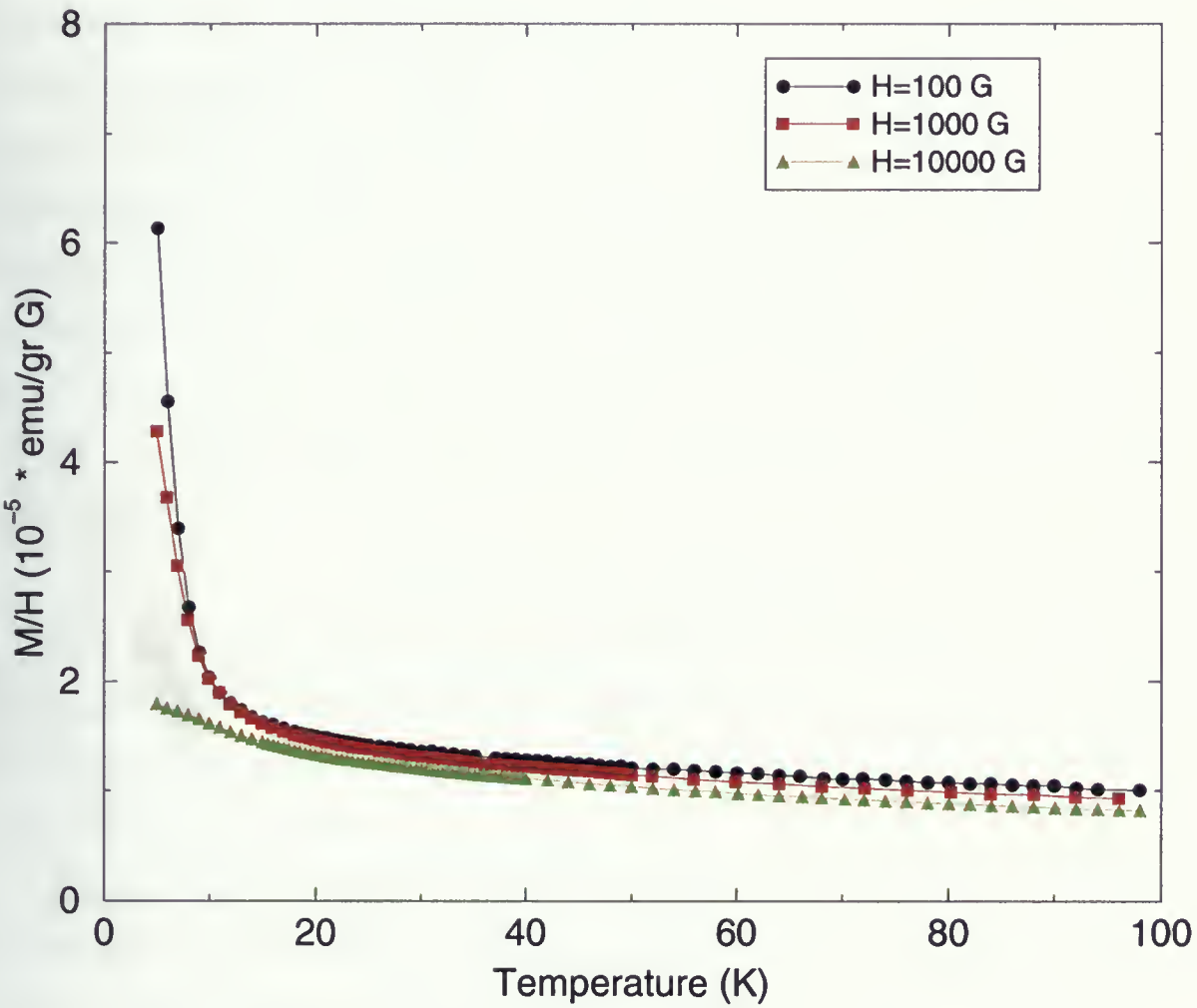

Figure 3.8: Magnetic susceptibility (χ) vs. Temperature for sample $Na_{0.7}CoO_2$ at different fields H=100 G, 1000 G and 10000 G.

ing properties of fully hydrated sample $Na_{0.35}CoO_2 \cdot (4/3)H_2O$ were characterized by DC susceptibility using SQUID magnetometer. Fig. 3.11 shows the magnetic susceptibility (χ) of $Na_{0.35}CoO_2 \cdot (4/3)H_2O$ as a function of temperature. In the measurements under the external field of 10 G, T_c was about 4.2 ± 0.1 K for both *ZFC* and *FC* processes. In Fig. 3.12, magnetic susceptibility (χ) was measured under low fields between 10 G to 200 G by the step of 10 G, by the zero field cooling process. For the fields greater than 150 G, magnetic susceptibility was not negative down to 2.5 K. However, superconducting transition was observed by the downturn of χ although it was quite broad. The lower critical field H_{C1} can be determined from M-H curves for fields lower than 200 G as shown in 3.9. Magnetization is field dependent and by applying field below H_{C1} tries to deviate from the straight line at H_{C1}. The $H_{C1}(0)$ value can be obtained by fitting the H_{C1}(T)-T (3.10) curve with the equation 3.6 [4].

$$H_{C1}(T) = H_{C1}(0)(1 - (T/T_C)^2) \tag{3.6}$$

Using equation 3.6 has resulted the value of $H_{C1}(0)$=66 G and T_C=4.12 K. There are some arguments about fitting parameters H_{C1}(T) and T_C. Sakurai *et al.* [55] found H_{C1}=28.1 Oe and T_C=4.59, Takada *et al.* [4] reported H_{C1}=100 Oe and Badica *et al.* [56] reported the H_{C1}=17 Oe and T_C=3.8 K.

.Fig. 3.13 shows susceptibility measurements for fully hydrated sample $Na_{0.35}CoO_2 \cdot (4/3)H_2O$ and non superconductor sample $Na_{0.35}CoO_2$. The fully hydrated sample has a larger total susceptibility and it may result from a change in χ_{VV} and χ_{pauli} from Eq. 3.3, although it is not possible to separate these two terms independently. Around 45 K, an anomaly appears for both samples which it is due to residual oxygen on the surface or in the intercalated water on the sample.

[4] [54]

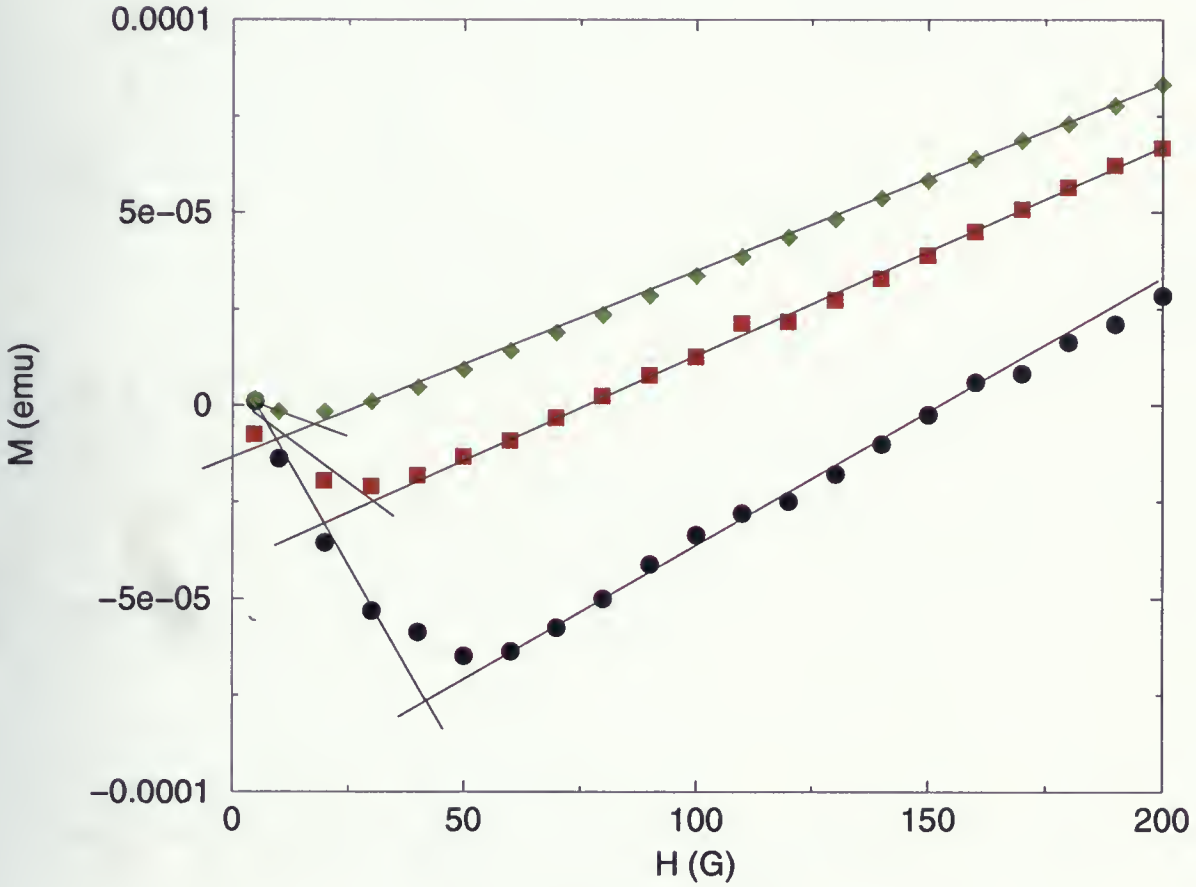

Figure 3.9: Magnetic moment (*emu*) vs. Field.

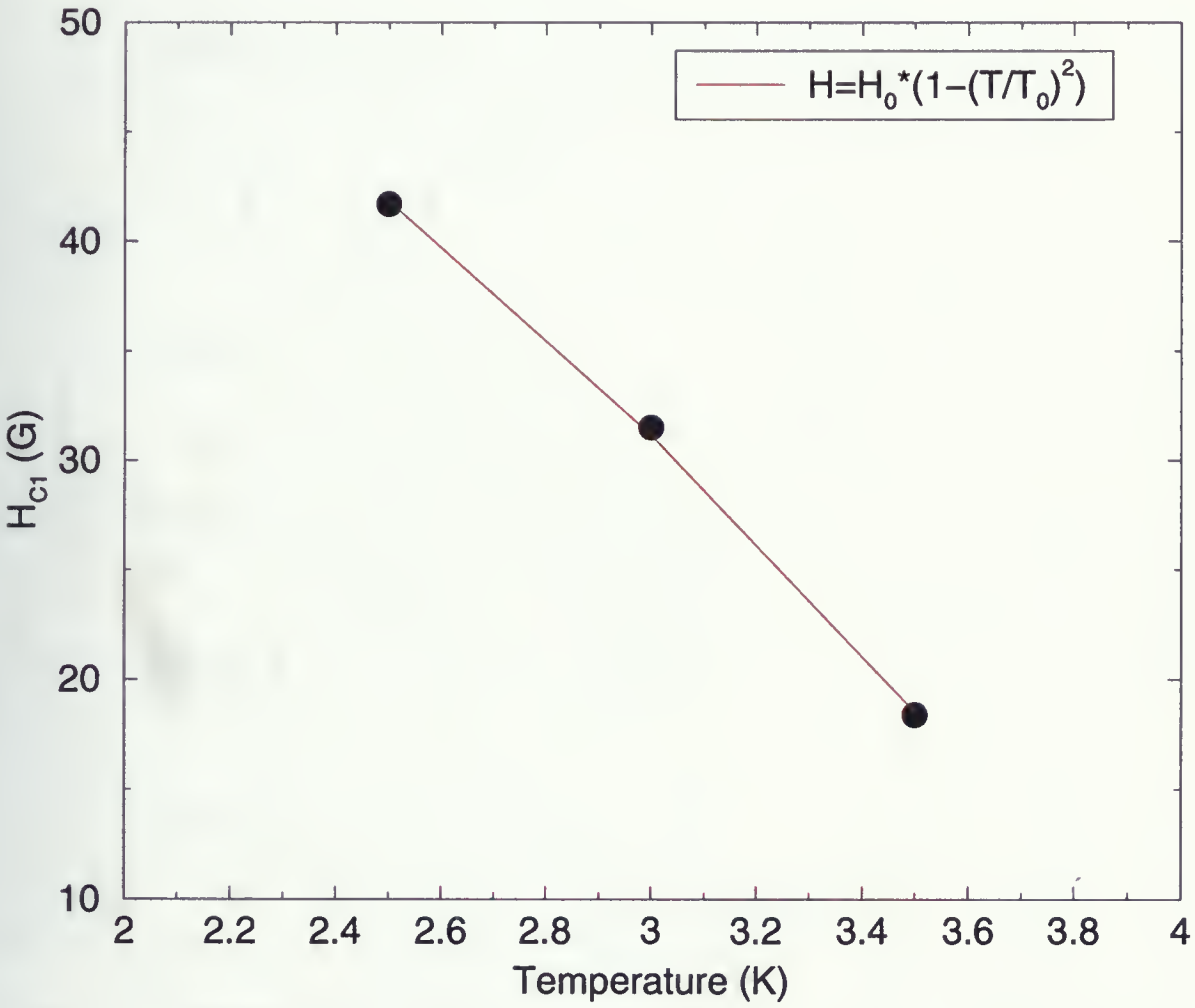

Figure 3.10: Critical magnetic field (G) vs Temperature.

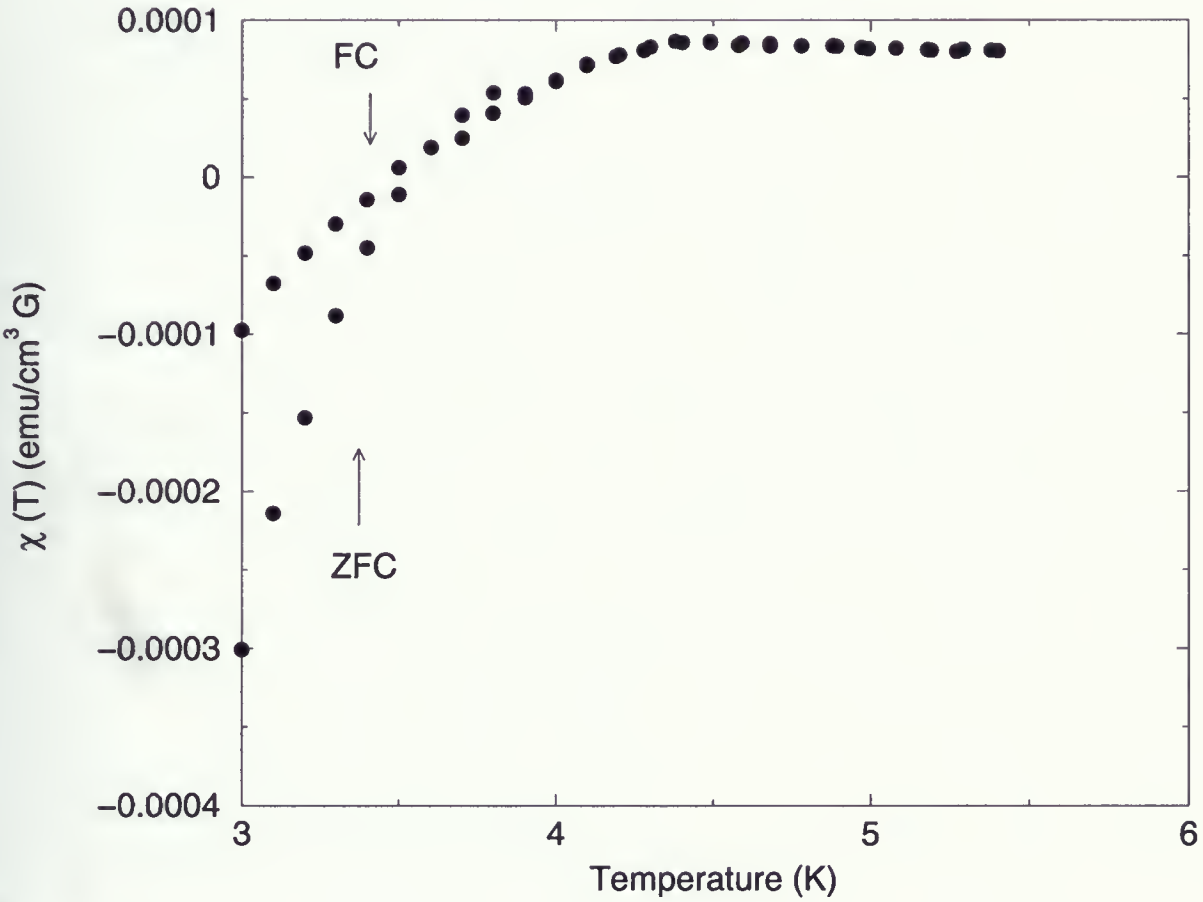

Na

Figure 3.11: Magnetic susceptibility vs. Temperature (χ) of $Na_{0.35}CoO_2 \cdot (4/3)H_2O$. FC and ZFC is shown with arrows. External field of H=10 G was applied.

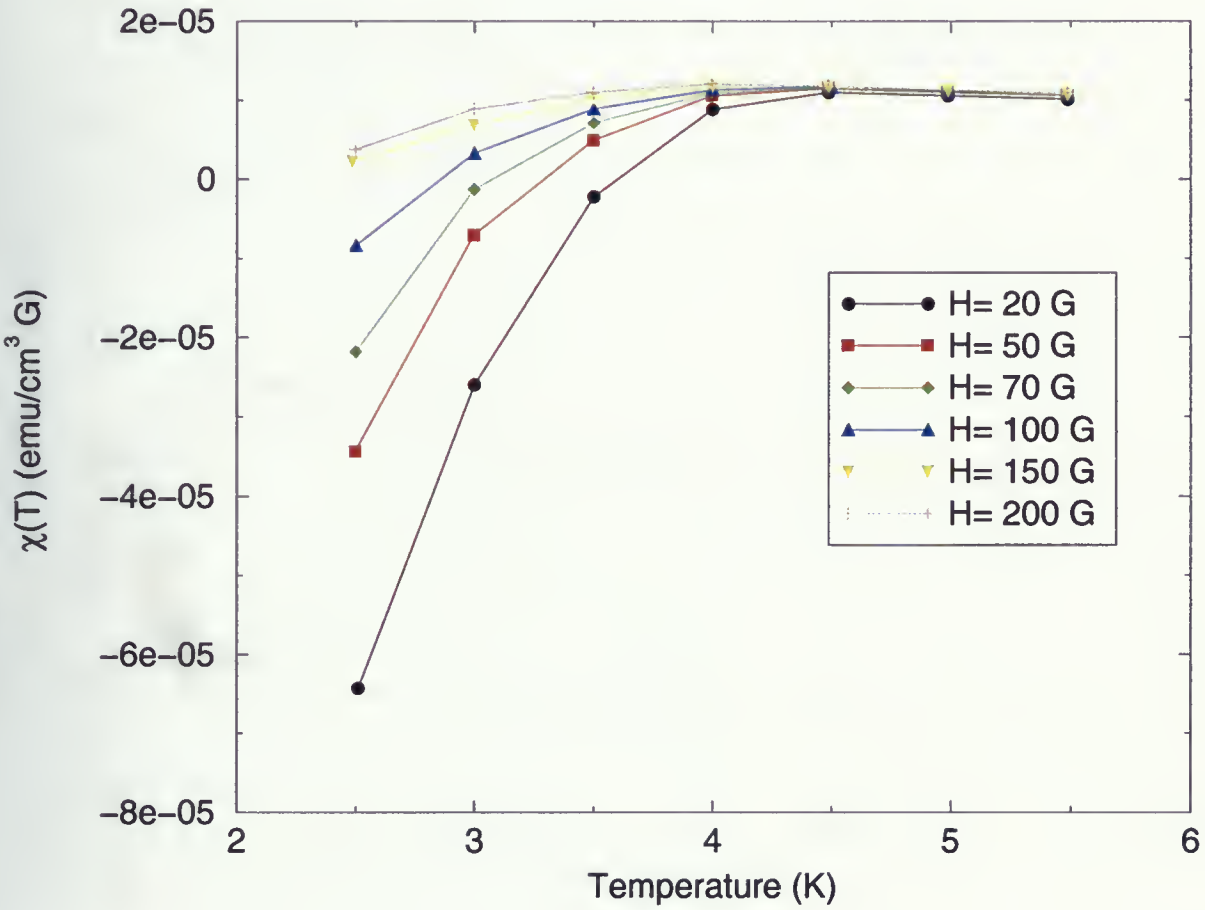

Figure 3.12: Magnetic susceptibility (χ) vs. Temperature. Different fields was applied in FC process.

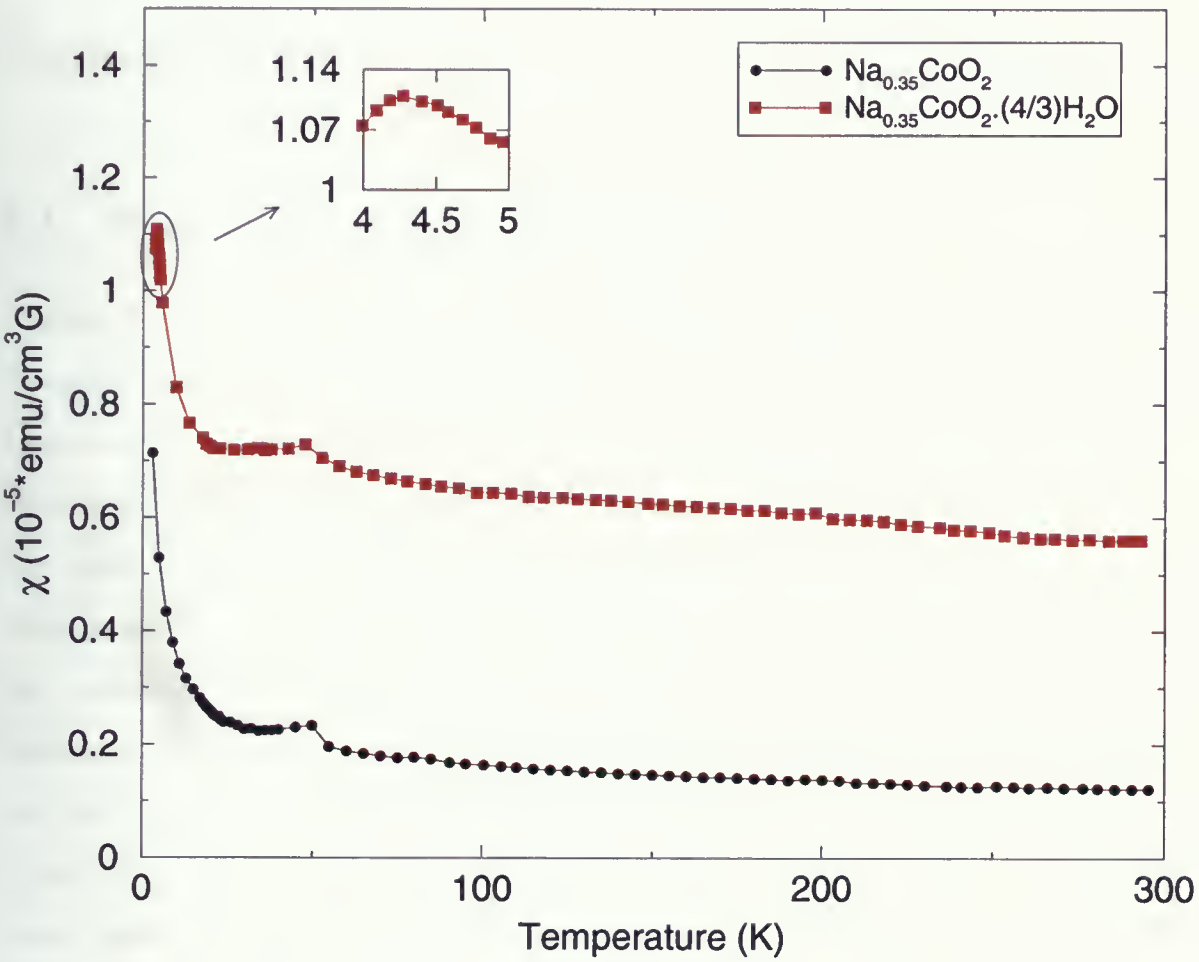

Figure 3.13: Magnetic susceptibility (χ) vs. Temperature for sample fully hydrated sample $Na_{0.35}CoO_2 \cdot (4/3)H_2O$ and non superconductor sample $Na_{0.35}CoO_2$. Magnetic field H=100 G was applied. Inset shows the superconducting transition.

Chapter 4

Resistivity

4.1 Four probe resistance measurements

The four point probe method is typically used to determine bulk resistivity. When a simple measurement of the electrical resistance is performed by attaching two wires to it, the resistance of the contact point of the wires to the sample is also measured. Typically the resistance of the point contact (called contact resistance) for a sample with large resistance is very small thus it can be ignored. However, when one is measuring a very small sample resistance, especially under variable temperature conditions, the contact resistance can dominate and completely obscure changes in the resistance of the sample itself. The effect of contact resistance can be eliminated with the use of a four point probe method. A schematic of a four point probe is shown in Fig. 4.1. In this diagram four wires (or probes) have been attached to the test sample. A constant current is made to flow the length of the sample through probes labeled a and d in figure 4.1. This can be done using a current source or a power supply as shown. If the sample has any resistance to the flow of electrical current, then there will be a potential (or voltage) drop as the current flows along the sample. To eliminate the thermal voltage, each data point was calculated from the difference between voltage as direct and reversed polarity of the current source and the results are averaged;(V=(V_+-V_-)/2)and R=V/I. Therefore, R between b and c is determined using an average of the two voltages and the applied current [57].

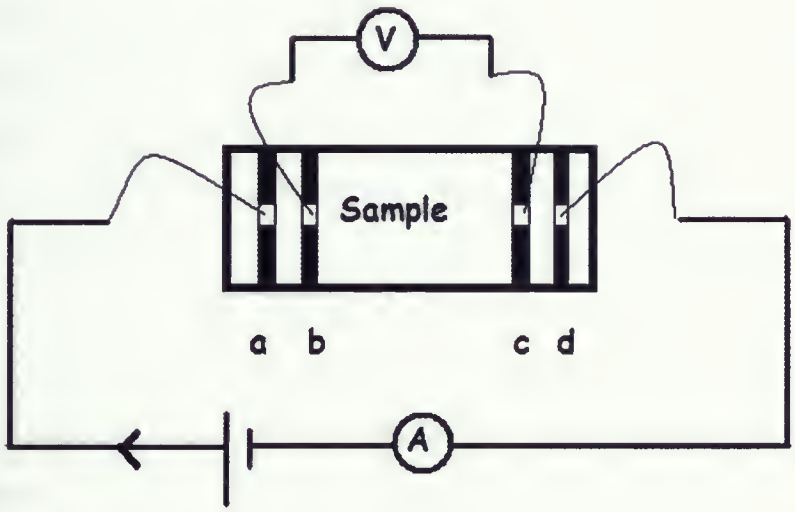

Figure 4.1: Schematic diagram of the four-probe technique. Resistance of the sample for each temperature was calculated from the difference between voltage as direct and reversed polarity of the current source and the results are averaged;(V=(V_+-V_-)/2)and R=V/I. Therefore R between b and c is determined using an average of the two voltages and the applied current

4.2 Preparation for Resistivity measurement

The resistivity measurements were performed on the samples with rectangular shape with dimensions of approximately $5\ mm * 2\ mm * 2mm$. Since Na_xCoO_2 is sensitive to moisture in the ambient atmosphere, silver paste was not good for making connection between sample and gold wires. Gold evaporation was used to make four strips of a thin layer of gold on the sample's surface. Fig. 4.1 is a schematic of the sample which is ready for measurement. Turbo molecular pump was used for making vacuum up to 10^{-6} Torr and cryostat cooled samples from room temperature down to 14 K. As it was mentioned in Chapter 2, resistivity measurements for all the samples annealed in flowing Argon show insulating behavior. Fig. 4.2 shows temperature dependence of resistivity for the sample $Na_{0.75}CoO_2$ which was annealed in flowing Argon. Fig. 4.3 shows resistivity of Na_xCoO_2 where $x = 0.4, 0.5, 0.7, 0.8$. From room temperature down to 14 k. All the samples show metallic behavior (*i. e.* $d\rho/dT > 0$) in the whole temperature range studied. Since X-ray measurements showed that these samples are all $Na_{0.7}CoO_2$ with different kinds of impurities, strange resistivity behavior is not unexpected. Also there is a kink observable for sample $Na_{0.7}CoO_2$ at around 280 K, which will be discussed later on in this chapter.

4.3 Magnetoresistance

Magnetoresistivity (MR) is the change in electrical conductivity when a magnetic field (H) is applied. The change of the resistance is usually proportional to H^2 for small fields, however, at high fields it can rise faster than H^2 [58]. Measurements at lower temperature were performed by inserting the probe into the automatic Quantum Design Magnetic Properties Measurement System (MPMS). The MPMS system consists of the Helium dewar with a superconducting magnet, SQUID detection system and probe assembly connected to control

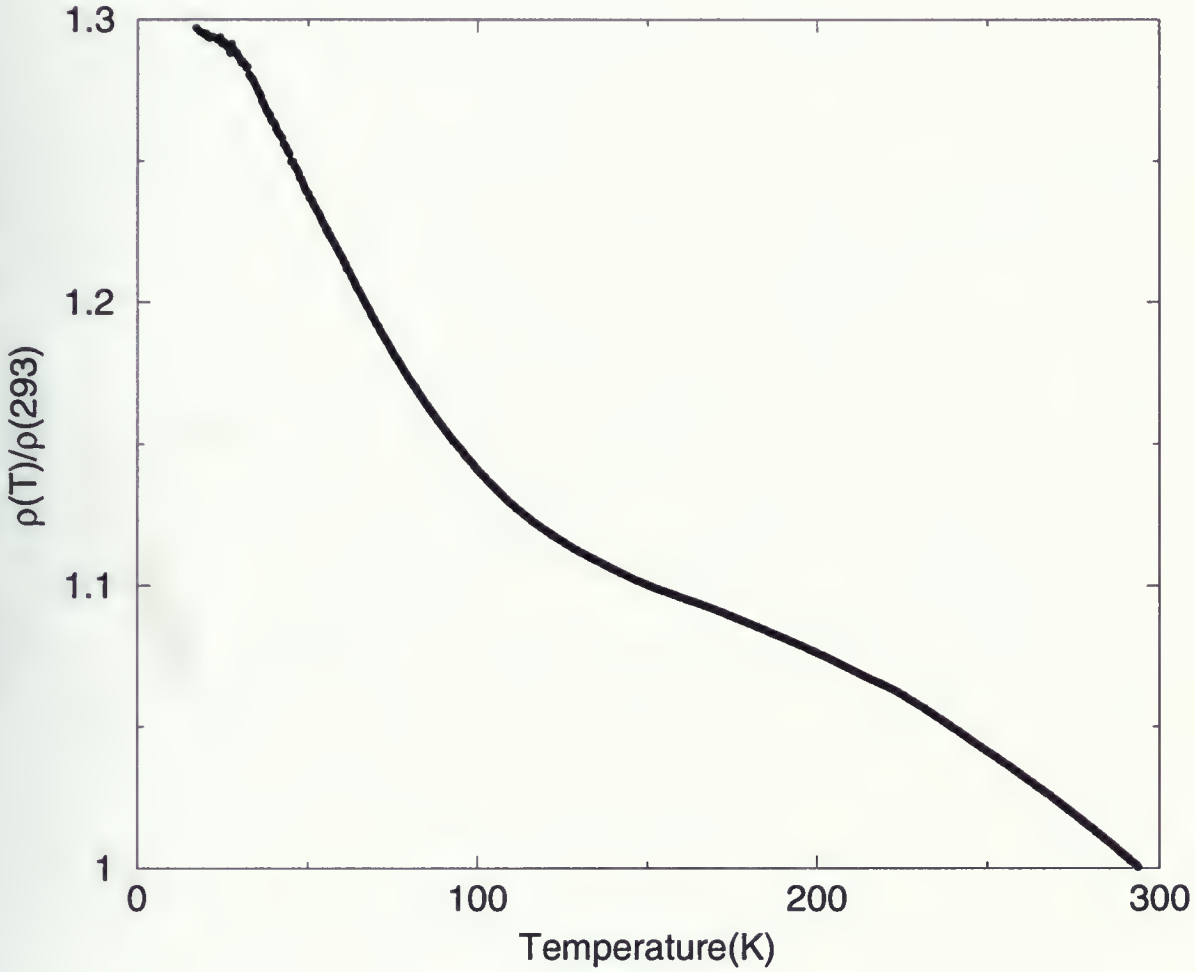

Figure 4.2: Resistivity measurement of $Na_{0.75}CoO_2$ annealed with Argon

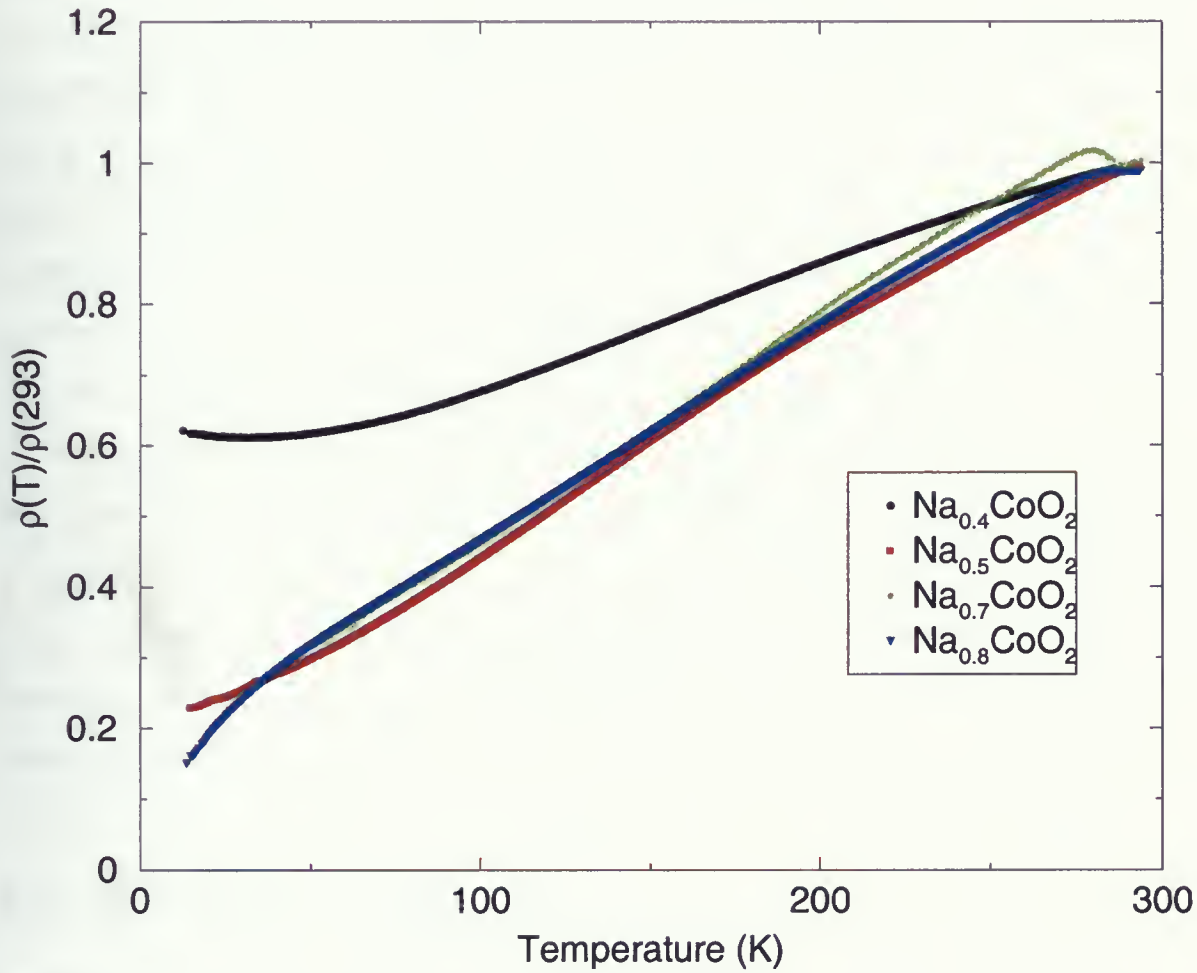

Figure 4.3: Resistivity measurement of Na_xCoO_2 with different concentration of Na

systems. Automatic control and data acquisition are performed using a PC computer and subsystem controllers [59]. The magnetoresistance was measured as a function of temperature by using a current of 1 mA. Data were collected by switching current in every 0.5 temperature interval while constant field had been applied. Four probe contact was used for measurement. Measurement has been done for sample $Na_{0.7}CoO_2$ where temperature changed from 5 K to 320 K and fields were H=10 G, 30 kG and 55 kG[1], and as it is shown in Fig. 4.4. Since there was not any appreciable change between H=10 G and H=30 kG; H=55 kG was applied to see if a higher field can make any difference. A small change was observed between H=30 kG and H=55 kG but mostly at low temperatures. Fig. 4.5 shows the temperature dependence of $\delta\rho_H/\rho_0$ between 5 K and 50 K. From Fig. 4.5, MR has greater magnitude in higher field. Above 20 K, the MR values are close to zero.

Two previous groups have reported the increase in resistivity at 2 K, by applying magnetic field of 80 kG and 70 kG [60, 61, 62]. Motohashi *et. al.* [34, 63] showed that the difference in the MR effect is more significant at lower temperatures. The $Na_{0.75}CoO_2$ sample showed a large positive MR at 5 K. They also showed that MR value at 7 T abruptly increased. The onset temperature of the MR effect was at T_m=22 K, which they corresponded this T_m to SDW transition.

4.4 Hydrostatic pressure

Pressure is a controllable and reversible experimental parameter that can be changed over a wide range to probe the properties of condensed matter systems. Applying pressure makes it possible to bring a system near the structural, electronic and other kinds of phase transitions. Such changes often take place at very low temperature and frequently involve the use of magnetic fields. But there is some limitation in the strength of even the strongest materials.

[1]There is around 30% error in low field due to the remenant magnetic field.

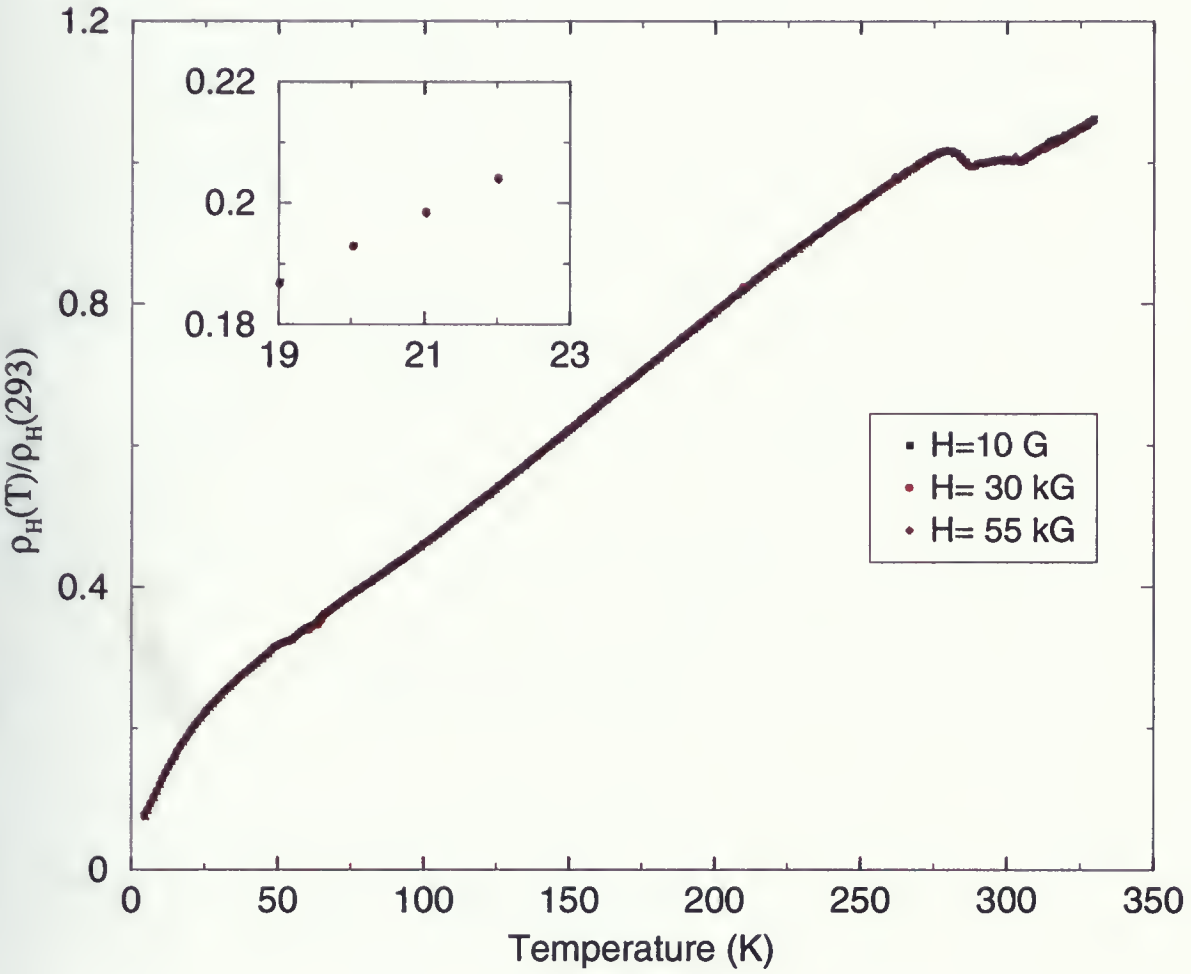

Figure 4.4: Magnetoresistivity measurements for sample $Na_{0.7}CoO_2$. Fields H=10 G, 30 kG, 55 kG was applied.

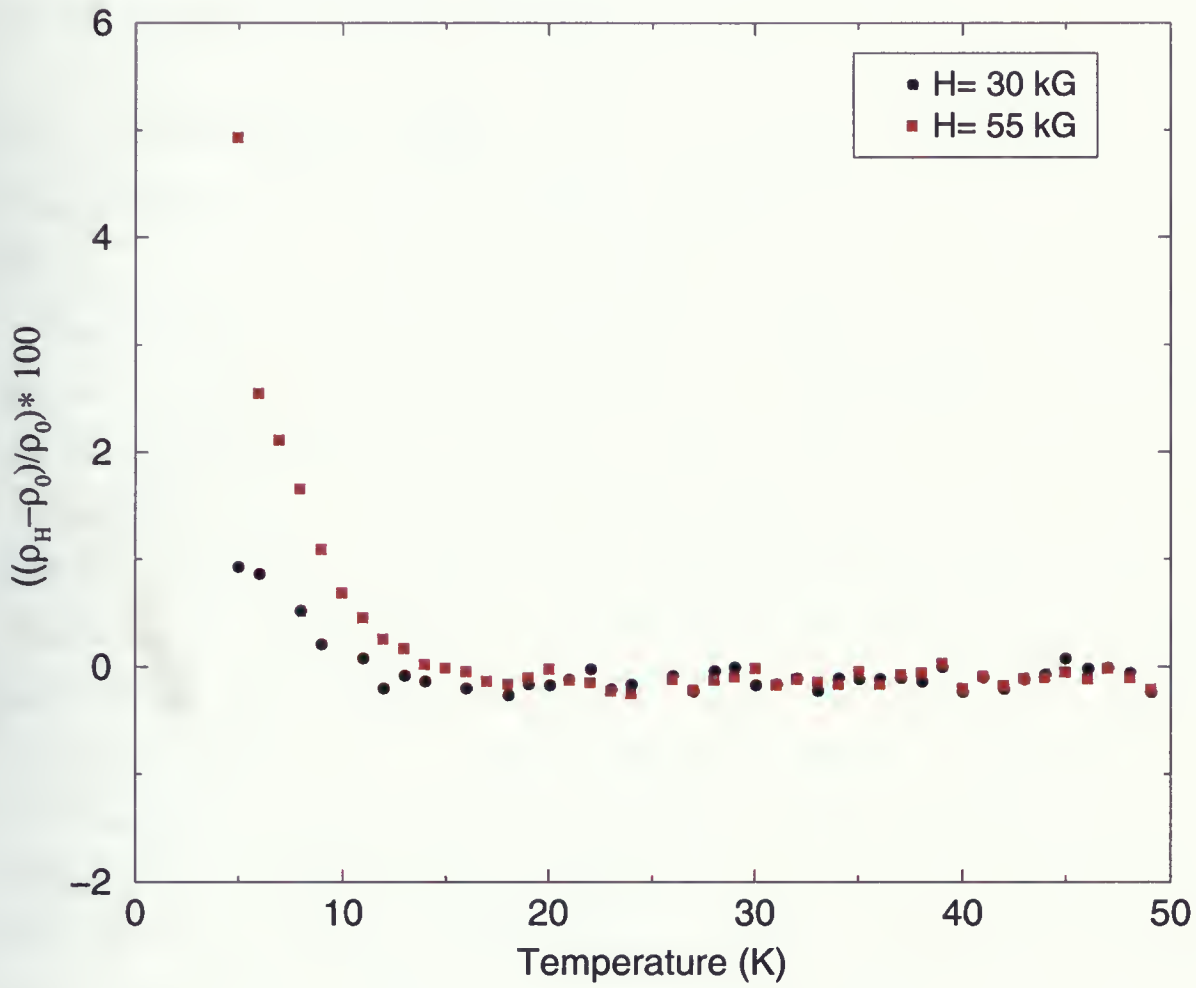

Figure 4.5: Magnetoresistivity measurements for sample $Na_{0.7}CoO_2$. ρ_H is the resistivity where field H is applied and ρ_0 is resistivity where 10 G field was applied.

For instance the highest pressure which can be applied is about 50 kbar and it requires the anvil pressure cells, such as diamond anvil and sapphire anvil cells. However, the limited amount of space in such devices is often a great inconvenience, and for lower pressures it is very useful to be able to employ piston cylinder cells [64].

4.4.1 Measurements under hydrostatic pressure.

Pressure effects were measured using a self-clamping type pressure cell, which shown in Fig. 4.6.

Force is applied to the pressure cell at room temperature by a conventional lab press. The force is transmitted to the sample region, which is located under the nylon cap, (Fig 4.6 and 4.7), through a tungsten-carbide piston.

The applied pressure is transmitted to the sample through the transmitting medium which is silicon oil in this case. The pressure in the cell was determined at all temperatures using the known pressure dependence of the resistance of a lead sample which is located under the same nylon cap, close to the sample, figure 4.7. In other words, the lead strip is an internal pressure manometer. It is important to have lead, because the pressure is reduced as the temperature is lowered, which results in the thermal contraction of the pressure transmitting medium. To account for this problem, resistance dependence of the pressure for the calibrated lead strip was fitted with polynomial equation and constants were obtained [66]. Each time the cell was pressurized, resistance of the sample and lead were measured for different temperatures. Using the polynomial equation with known constants enables to determinnation of the actual pressure from a lead resistance and use it for plotting pressure dependence of resistivity for the sample.

The resistance of the sample $Na_{0.7}CoO_2$ was measured using four probe contact method. In this technique, a thin gold wire is soldered to each of the four gold thin films on the

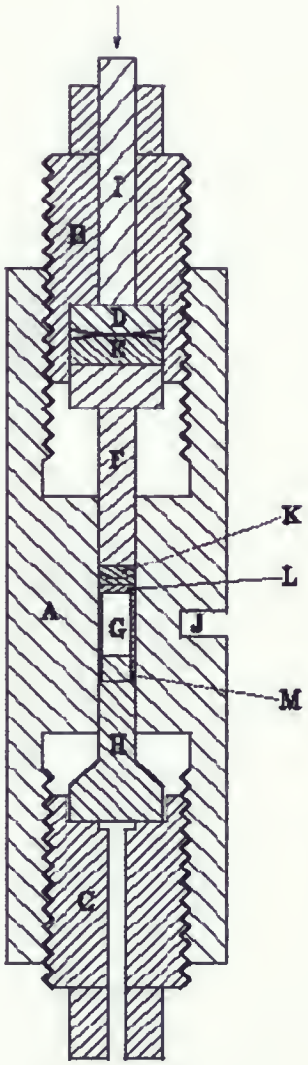

Figure 4.6: Schematic diagram of Hydrostatic pressure cell for resistivity measurements: A body of cell (CuBe); B,C-tightening nuts (CuBe); D,E -springs (CuBe); F-plug (CuBe/WC); J-thermometer area; K-protecting washer (CuBe/Teflon); L-nylon container; M-washer (CuBe). The arrow indicates where the force is applied [65]

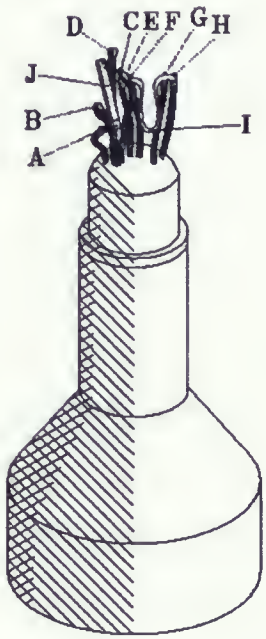

Figure 4.7: Schematic diagram of Hydrostatic pressure cell with sample for resistivity measurements. A, B, C, D connected to the samples and E, F, H and connected to lead [65].

sample; using Indium. As shown in Fig. 4.1, first Indium is melted onto the gold thin film, and then a gold wire is laid down on the Indium spot and soldered with Indium. The gold wires are then soldered to Cu wires. The four contacts were labeled as A, B, C and D. A constant current of 1 mA is applied between points A and D, and voltage between B and C is measured using a nanovoltmeter. The pressure cell is placed inside a 3-layered cryostat, Fig. 4.8. Chambers A and C of the dewar are connected to a turbomolecular pump to hold a high vacuum. Chamber B is used for liquid Nitrogen. Their function is to insulate the inner chamber D from the outer environment. The pressure cell, connected to a supporting rod, is inserted in the chamber D, which can be hermetically closed on the top. The temperature is monitored by a thermometer inside the cell. The middle and inner dewar (chamber B and D in Fig. 4.8) are filled with liquid Nitrogen [67]. At temperature 77 K, liquid Nitrogen in the inner dewar (chamber D) is replaced by liquid Helium. The pressure cell is allowed to cool down to around 4.2 K, then measurements were taken as the system slowly warms up.

Measurements were carried out at ambient pressure from 4.2 K to 293 K. The value of resitivity at room temperature was the order of 1-10 $m\Omega cm$. This value is in reasonable agreement with several other reports of resistivity measurements made on either polycrystalline sample or single crystal samples of $Na_{0.7}CoO_2$ in the *ab* plane [2, 9, 34, 61, 62, 68]. Temperature dependence of resistivity for the sample $Na_{0.7}CoO_2$ in a zero pressure followed the same path as magnetoresistance measurement. The anomaly which was seen in earlier measurements (resistivity and magnetoresistivity; Fig. 4.4 and 4.5) between 260 K-290 K, can also be seen in Fig. 4.9. This anomaly is a first order transition and appeared in all measurements and it has been reported by different groups [15, 37, 61, 69, 39]. Sales *et al.* [37] measured three samples of $Na_{0.75}CoO_2$ one of which was polycrystalline and the other two were single crystals. Using scanning calorimetery data (DSC), a peak was detected at 343 K for the floating zone grown crystal and at 430 K for the flux grown crystal and between 250 K-310 K for the polycrystalline sample. From X-ray and neutron diffraction studies, it

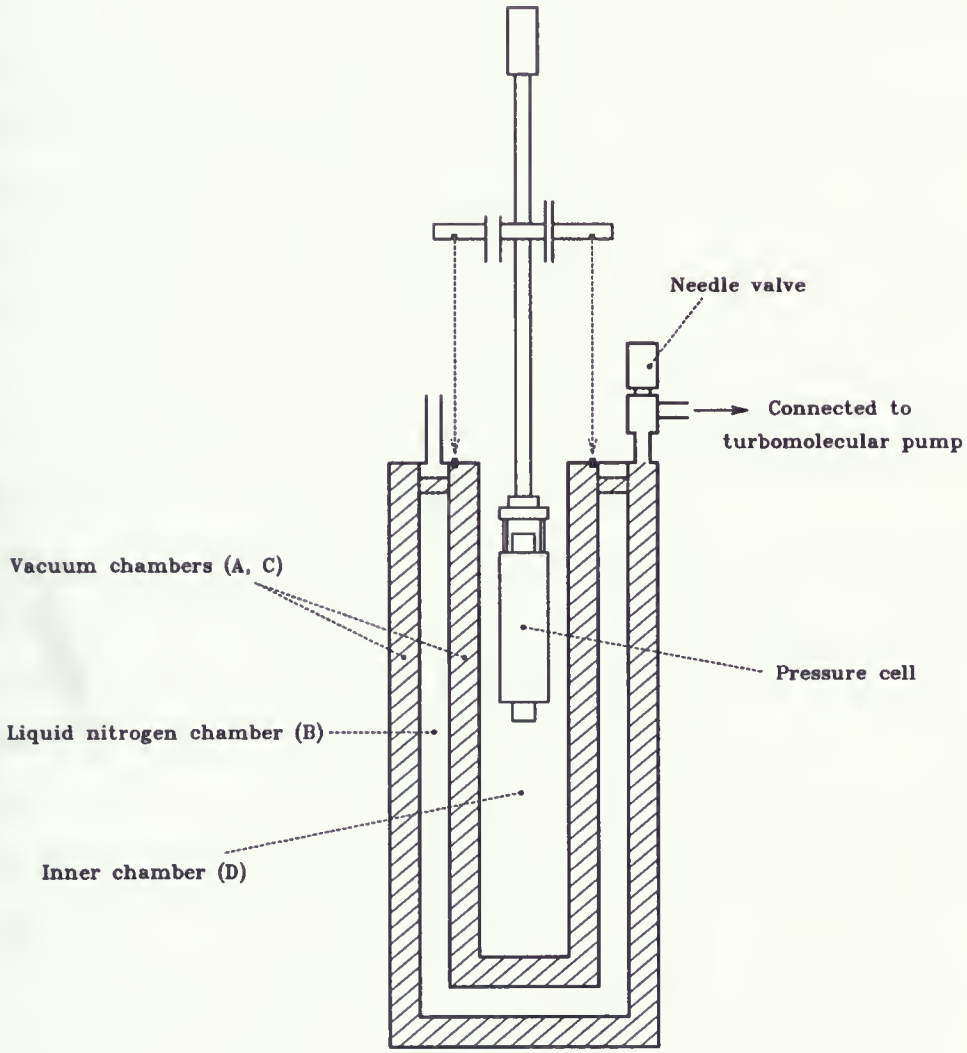

Figure 4.8: Cryostat [65]

is reported that this anomaly is most probably due to the rearrangement of the Na between CoO_2 layers [2, 24, 37, 39, 70]. At high temperature Na ions are able to move through the planes between the two oxygen sheets. Thus, ionic conduction is expected via the direct movement of the sodium ions. The sodium atom can occupy two positions in the lattice and freezing of the sodium in one of the positions can cause a small increase in resistivity [23, 61].

For the sake of comparison all sets of data are normalized with their resistivity value at room temperature R(293), with results shown in Fig. 4.10. Applying pressures of 3 kbar and 5 kbar, have not affected transition temperature between 275 K and 280 K. However, applying higher pressure (8 kbar) made the transition sharper.

Fig. 4.11 shows pressure dependence of the resistivity at room temperature, when it is observed that as pressure is increased, room temperature resistivity decreases at a rate $d\rho/dp = -0.033 \pm 0.76 * 10^{-4}(m\Omega cm/kbar)$.

In order to see the effect of the pressure on the magnetic transition at low temperatures, resistivity measurements were performed at three different pressures of 0, 5 and 11 kbar. Fig. 4.12 shows resistivity behavior in the temperature range of 4 K to 230 K. The resistance ratios ($R_{293\ K}/R_{4\ K}$) for applied pressures of 0, 5 and 11 kbar were 13.28, 15.07 and 16.56, respectively. Bayrakci *et al.* [71] reported this ratio as 20 for the single crystal sample with Na concentration of 0.82. It was found that the resistivity between 230 K and 40 K varies almost linearly with temperature by $d\rho/dT = 14.9 \pm 4.7 * 10^{-3}$ and $14.2 \pm 6 * 10^{-3}$ and $14 \pm 8.7 * 10^{-3}$ $\mu\Omega cm K^{-1}$ respectively. Below 40 k, this rate of change ($d\rho/dT$) increased by decreasing temperature and it had the maximum value at 8 K as shown in Fig 4.12. This marks the SDW transition as reported by other group [61, 72, 73]. It is noted that applying pressure decreased the transition temperature. The reduction in ρ below 40 K, suggests that opening up the gap associated with SDW, results in a decrease in the total scattering. This downward feature is reported in the literature [9, 34, 61].

It is noteworthy that the $d\rho/dT$ is decreased by applying pressure. The temperature

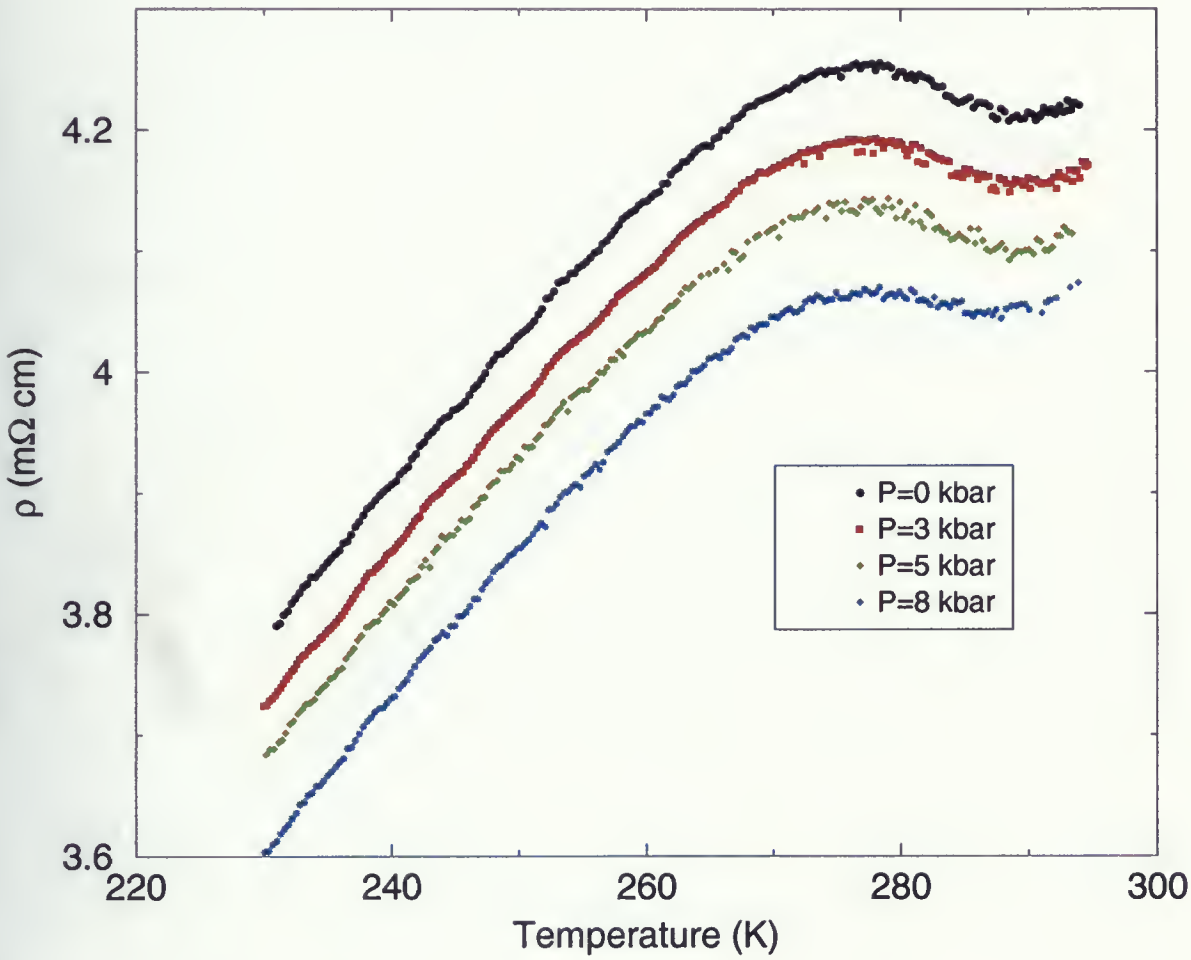

Figure 4.9: Pressure dependent resistivity for sample $Na_{0.7}CoO_2$ in temperature range of 230 K to 293 K

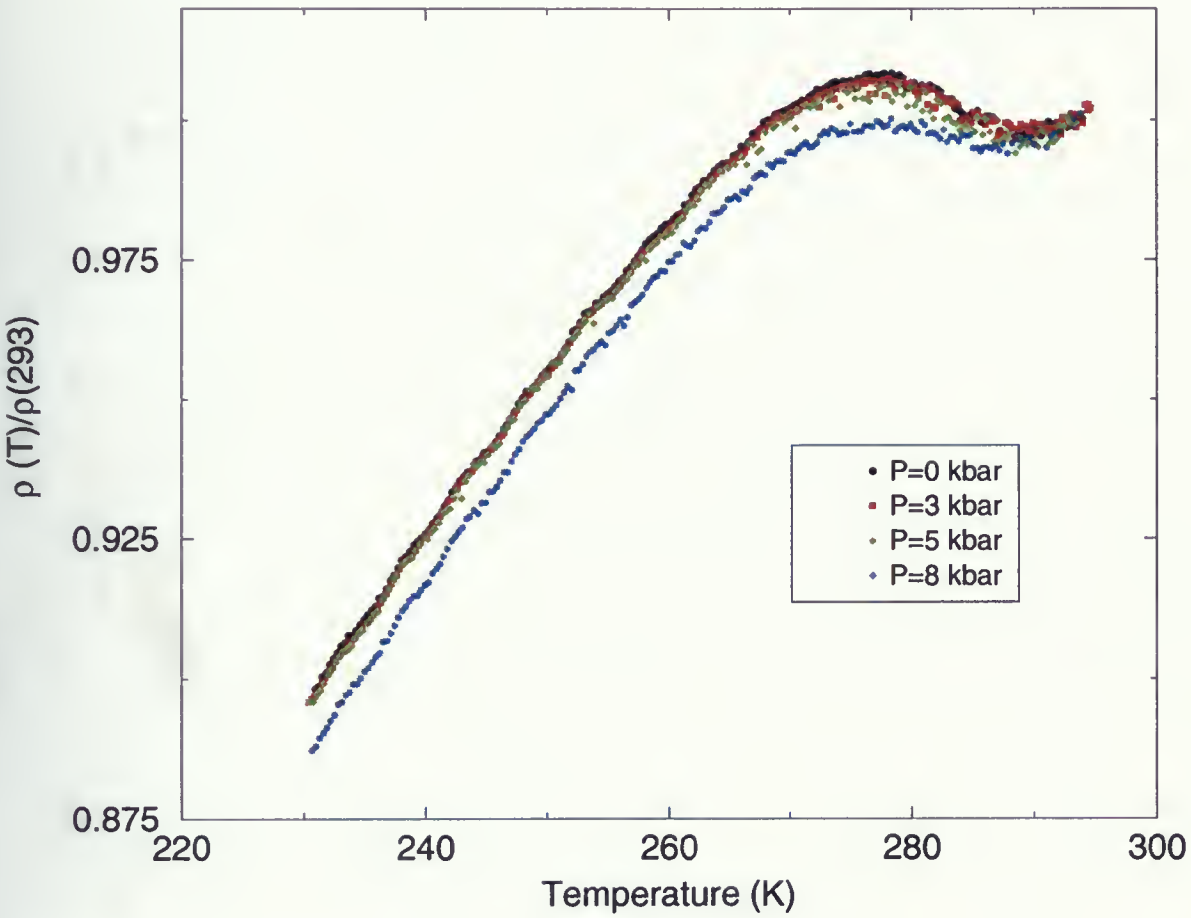

Figure 4.10: Pressure dependent resistivity for sample $Na_{0.7}CoO_2$ in temperature range of 230 K to 293 K

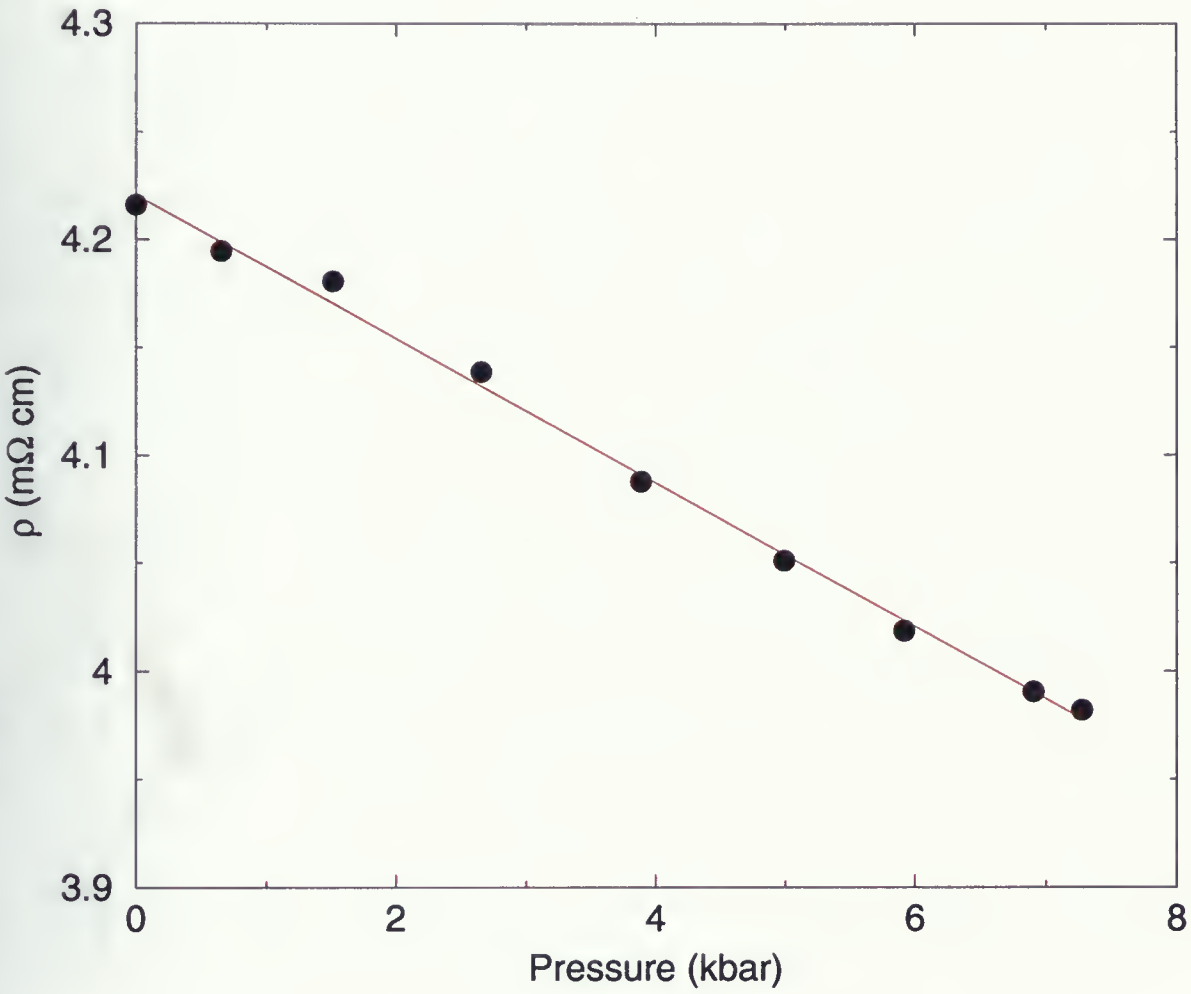

Figure 4.11: Pressure dependence of the resistivity for sample $Na_{0.7}CoO_2$ at room temperature T=293 $\pm$ 0.5 K. The slope is $d\rho/dp = -0.033 \pm 0.76 * 10^{-4}(m\Omega cm/kbar)$. Errors on pressures are around 0.01 kbar.

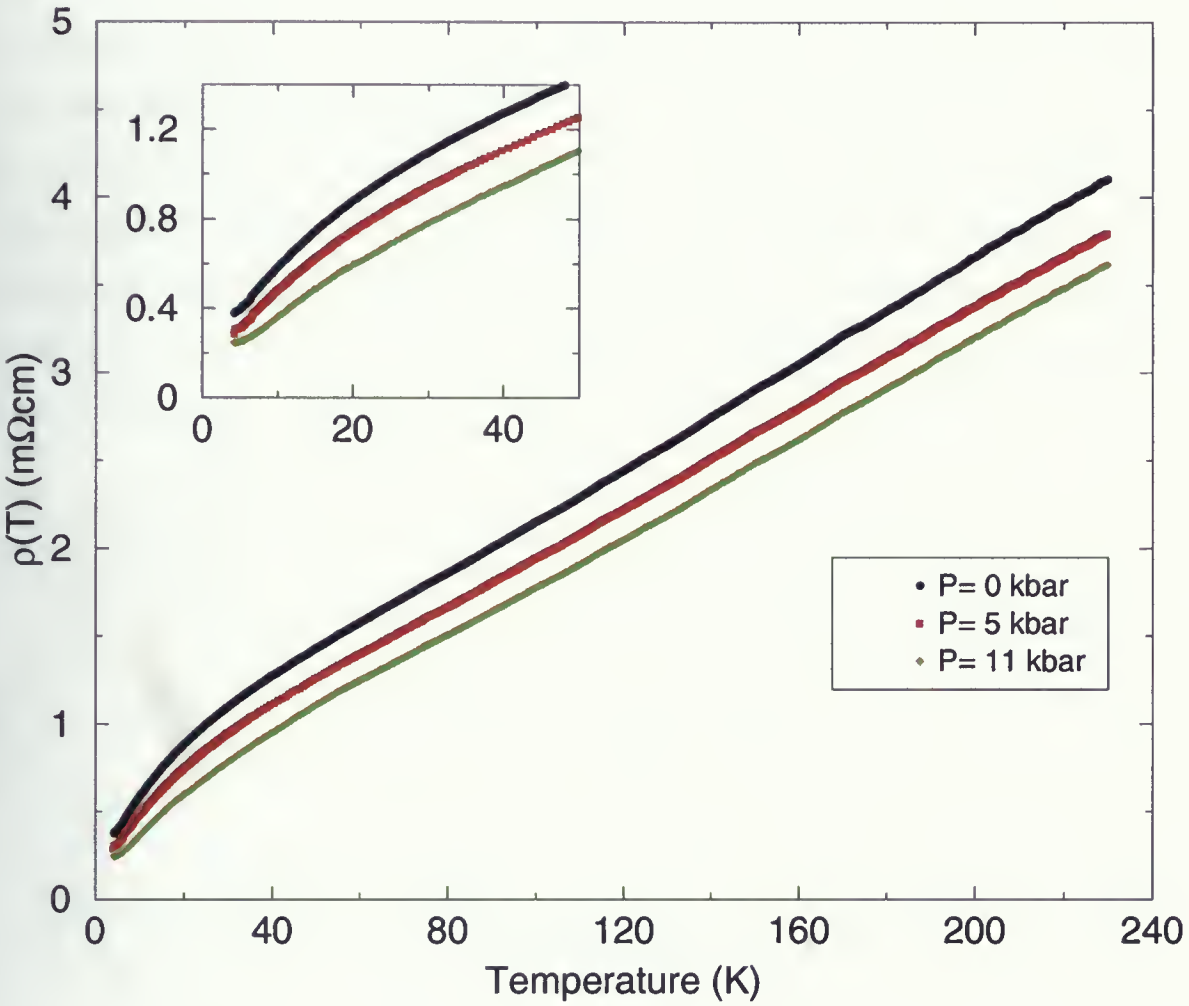

Figure 4.12: Pressure dependent resistivity for sample $Na_{0.7}CoO_2$ in temperature range of 4 K to 230 K. The inset shows temperature range of 4 K to 50 K, small kink at around T=8 K is indicated with arrow.

dependence of resistance (R(T)) at low temperature can be parametrized by a power law $R(T) = R_0 + AT^n$ over an extended temperature range up to 40 K [74]. In zero pressure R(T) is increasing with T, where power of T is n$\simeq$ 0.55. Applying pressure changes the rate of increasing to n$\simeq$0.6 for P=5.8 kbar and 0.68 for 11 kbar. Shi *et al.* [14] reported the n value as 0.42 for the temperatures below 40 K. Bruhwiler *et al.* [74] reported the value of n$\simeq$ 0.65-0.7 for zero field. This T-dependence indicates a low residual resistance, reflects a highly unusual and strong scattering of the charge excitations with a decreasing scattering towards zero temperature. Magnetic transition temperature T_{C1} decreased with pressure as shown in fig. 4.13. Change of T_{C1} with pressure is almost linear and the rate of the change is -0.15 K/kbar.

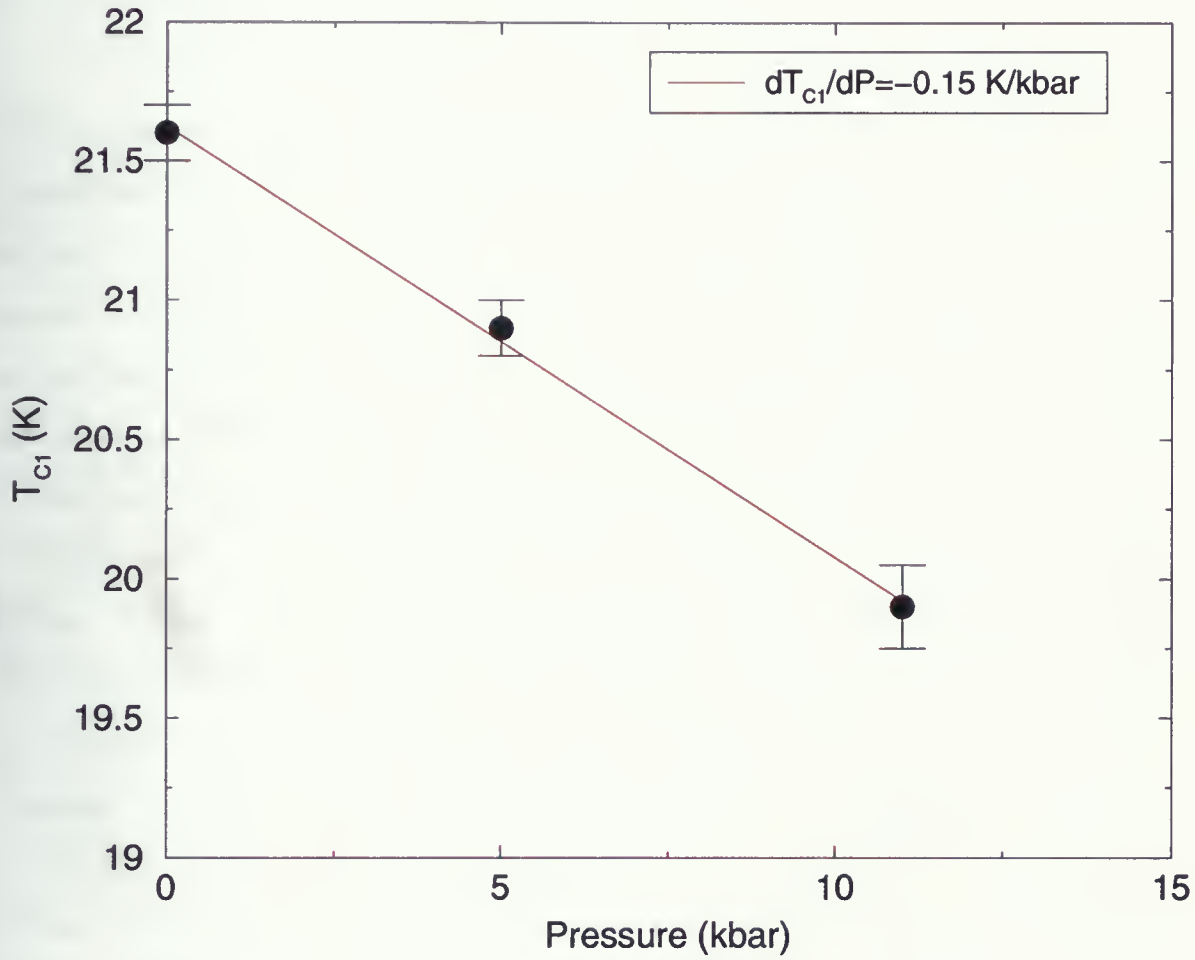

Figure 4.13: Pressure dependent transition temperature sample $Na_{0.7}CoO_2$.

Chapter 5

Conclusions

Two batches of samples of Na_xCoO_2 with $x = 0.25, 0.4, 0.5, 0.6, 0.7, 0.75$ were prepared using "Rapid heat-up" in flowing O_2 and Argon. Glassy layer was observed on the sample surface because of using this method. For the sample with Na concentration of 0.7, removing glassy layer enable one to get single phase polycrystalline. Resistivity measurements show an insulating behavior in Argon annealed samples, whereas O_2 annealed samples exhibit metallic behavior. X-ray powder diffraction data, for all concentrations of x have resulted in mixed phase samples containing Co_3O_4 and Na_xCoO_2 with $x \simeq 0.7$.

Magnetization and resistivity measurement of polycrystalline Na_xCoO_2 have revealed a number of features present over a range of Na doping. Magnetization showed a clear peak at 35 K which is due to the Co_3O_4 impurity. Magnetoresistivity measurements showed two transitions at T_1=22 K (magnetic transition) and T_2=280 K (structural transition). Transition at T_1=22 K showed up only in the low field of 25 G. Applying pressure decreased the resistivity of the sample and decreased the transitions at T_1 and made a significant change on the transition temperature at T_2. Applying pressure also decreased the resistivity of the sample at room temperature, which is due to the decrease of the lattice parameters.

Bibliography

[1] I. Terasaki and Y. Sasago. Large thermoelectric power in $NaCo_2O_4$ single crystals. *Phys. Rev. B*, 56:R12685–R12687, 1997.

[2] Y. Wang and N. S. Rogado. Spin entropy as likely source of enhanced thermopower in $Na_2Co_2O_4$. *Nature*, 423:425–429, 2003.

[3] B. G. Levi. Intriguing properties put sodium cobalt oxide in the spotlight. *Physics Today*, 56:15–18, Aug 2003.

[4] K. Takada, H. Sakurai, and E. Takayama Muromachi. Superconductivity in two-dimensional CoO_2 layers. *Nature*, 422:53–58, 2003.

[5] P. Lemmens, V. Gnezdilov, N. N. kovaleva, K. Y. Choi, H. Sakurai, E. Takayama-Muromach, K. Takada, T. Sasaki, F. C. Chou, C. T. Lin, and B. Keimer. Effect of Na content and hydration on the excitation spectrum of the cobaltite$NaCo_2O_4 \cdot H_2O$. http://arXiv.org/abs/cond-mat/0309186.

[6] T. Motohashi and E. Naujalis. Simultaneously enhanced thermoelectric power and reduced resistivity of $Na_xCo_2O_4$ by controlling na nonstochiometry. *Appl. Phys. Lett*, 79:1480–1483, 2001.

[7] A. Pushp. The phases of Na_2CoO_2, 2004. `http://guava.physics.uiuc.edu/~nigel/courses/463/Essays_2004/files/pushp.pdf`.

[8] B. Lorenz and J. Cmaidalka. Effect of hydrostatic pressure on the superconductivity in $Na_xCoO_2 \cdot yH_2O$. http://arXiv.org/abs/cond-mat/0304537, 2003.

[9] M. l. Foo, Y. Wang, and S. Watauchi. Charge-ordering, commensurability and metallicity in the phase diagram of layered Na(x)CoO(2). *Phys. Lett. B*, 92:247001, 2004.

[10] D. Prabhakaran and A. T. Boothroyd. Magnetic studies of polycrystalline and single-crystal Na_xCoO_2. http://arXiv.org/abs/cond-mat/0312493, 2003.

[11] M. N. Iliev and A. P. Litvinchuk. Raman phonons and ageing-related surface disorder in Na_xCoO_2. *Physica C*, 402:239–242, 2004.

[12] J. Sugiyama and J. H. Brewer. Electron correlation in the two-dimensional triangle of Na_xCoO_2. http://arXiv.org/abs/cond-mat/0310637, 2003.

[13] Mukhamedshin. 23Na NMR evidence for charge order and anomalous magnetism in Na_xCoO_2. http://arXiv.org/abs/cond-mat/0402074, 2004.

[14] Y. G. Shi and H. C. Yu. Superstructure, sodium ordering and antiferromagnetism of Na_xCoO_2 (0.75¡x¡1). http://arXiv.org/abs/cond-mat/0401052, 2004.

[15] C. Bernhard and A. V. Boris. Charge ordering and magneto-polarons in $Na_{0.82}CoO_2$. http://arXiv.org/abs/cond-mat/0403155, 2004.

[16] T. Takeuchi and M. Matoba. Magnetic anomalies in Na_2CoO_2 (x=0.75). *Physica B*, 312–313:719–720, 2002.

[17] `http://www.chemistryquestion.com/English/Questions/SpecialistChemistry/9_solid_reaction_m`

[18] R. E. Schaak and T. Klimczuk. Superconductivity phase diagram of $Na_xCoO_2 \cdot 1.3H_2O$. *Nature*, 424:527–531, 2003.

[19] M. l. Foo and R. E. Schaak. Chemical instability of the cobalt oxyhydrate superconductor under ambient conditions. http://arXiv.org/abs/cond-mat/0304464, 2003.

[20] F. C. Chou, J. H. Cho, P. A. Lee, and E. T. Abel. Thermodynamic and transport measurements on superconducting Na_xCoO_2+yH_2O single crystals prepared by electrochemical de-intercalation. http://arXiv.org/abs/cond-mat/0404432, 2003.

[21] S. Park and Y. Lee. Novel synthesis and high pressure behavior of Na0.3CoO2x1.3H2O and related phases. http://arXiv.org/abs/cond-mat/0308353, 2003.

[22] Q. Huang, B. Khaykovich, F. C. Chou, J. H. Cho, J. W. Lynn, and Y. S. Lee. Structural transition in Na_xCoO_2 with x near 0.75 due to na rearrangement. *Phys. Rev. B*, 70:134115, 2004.

[23] R. J. Balsys and R. L. Davis. Refinement of the structure of $Na_{0.74}CoO_2$ using neutron powder diffraction. *Solid State Ionic*, 93:279–282, 1996.

[24] J. D. Jorgensen, J. C. Burley M. Avdeev, D. G. Hinks, and S. Short. Crystal structure of sodium cobalt deuterate superconductor Na_xCoO_2.4xD_2O x$\simeq$ 1/3. *Phys. Rev. B*, 68:214517, 2003.

[25] C. R. Wiebe, 2004. Private communication .

[26] Xtal Nexus, NRC, CA, www.unige.cd/crystal/stxnews/nexus/index.htm .

[27] 2003. http://www-llb.cea.fr/fullweb/fp2k/fp2k_intro_whatis.html .

[28] http://www.ndted.org/EducationResources/CommunityCollege/MagParticle/Physics/MagneticMa

[29] http://hyperphysics.phyastr.gsu.edu/hbase/solids/magpr.html#c2.

[30] http://www.ncsu.edu/chemistry/das/magnetochem.pdf.

[31] http://www.fkf.mpg.de/keimer/Lecture/Magnetism/Magnetism_6.pdf.

[32] N. P. Ong and R. J. Cava. Electronic frustration on a triangular lattice. http://wwww.princeton.edu/ npo/cobaltate.html, 2004.

[33] R. Ray, A. Ghoshray, K. Ghoshray, and S. Nakamura. ^{59}Co NMR studies of $NaCo_2O_4$. *Phys. Rev. B*, 59:P9454, 1999.

[34] T. Motohashi, R. Ueda, E. Naujalis, T. Tojo, I. Terasaki, T. atake, M. Karpinnen, and H. Yamauchi. Unconventional magnetic transition and transport behavior in $Na_{0.75}CoO_2$. *Phys. Rev. B.*, 67:064406, 2003.

[35] K. Miyoshi, E. Morikuni, K. Fujiwara, J. Takeuchi, and T. Hamasaki. Mass enhanced fermi liquid ground state in $Na_{1.5}Co_2O_4$, 2004. http://arXiv.org/abs/cond-mat/0403028.

[36] Y. Ono, R. Ishikawa, Y. Miyazaki, and Y. Ishii. Crystal structure, electric and magnetic properties of layered cobaltite β $NaCo_2O_4$ single crystals. *Phys. Rev. B*, 56:R12685–R12687, 1997.

[37] B. C. Sales, R. Jin, K. A. Affholter, and P. Khalifah. Magnetic, thermodynamic and transport characterization of $Na_{0.75}CoO_2$ single crystals. *Phys. Rev. B*, 70, 2004.

[38] T. Tojo, H. Kawaji, and T. Atake. First-order phase transition $Na_{1.5}Co_2O_4$. *Phys. Rev. B*, 65:052105, 2002.

[39] J. L. Gavilano and B. Pedrini D. Rao. Unconventional charge ordering in Na_xCoO_2 below 300 k. *Phys. Rev. B*, 69, 2004.

[40] F. C. Chou, J. H. Cho, and P. A. Lee. Magnetic susceptibility study of hydrated and non-hydrated Na_xCoO_2+yH_2O single crystals. http://arXiv.org/abs/cond-mat/0404061, 2004.

[41] Brian D. Josephson. Nobel prize, 1973. http://nobelprize.org/physics/laureates/1973/.

[42] James W. Rohlf. *Modern Physics from a to ZO.* Wiley, Wiley, 1994.

[43] The squid magnetometer, 2004. http://www.utoronto.ca/ phys325/exp04/squid.htm.

[44] Introduction to: AC suceptibility. Quantum Design, AC Susceptibility.

[45] Application notes/Technical advisories, quantum design .

[46] J. Sugyiyama, H. Itahara, and J. H. Brewer. Static magnetic order in $Na_{0.75}CoO_2$ detected by muon spin rotation and relaxation. *Phys. Rev. B*, 67:214420, 2003.

[47] G. Gaimi and L. Degiorgi. Ptical evidence for the proximity to a spin-density-wave metallic state in $Na_{0.7}CoO_2$. http://arXiv.org/abs/cond-mat/0404400, 2004.

[48] A. K. Cheetham and P. Day. *Solid state chemistry techniques.* Oxford science publications, US, NY, 1987.

[49] T. Waki, C. Michioka, and M. Kato. ^{59}Co NMR studies of $NaCo_2O_4$. http://arXiv.org/abs/cond-mat/0402503.

[50] T. Fujimoto, G. Zheng, and Y. Kitaoka. ^{59}Co NMR studies of $NaCo_2O_4$. *Phys. Rev. Lett*, 92:047004, 2004.

[51] Y. Kobayashi, M. Yokoi, and M. Sato. ^{59}Co NMR studies of $NaCo_2O_4$. *J. Phys. Soc. Jpn*, 72:2161, 2004.

[52] G. Baskaran. Electronic model for CoO layer based systems: Chiral resonating valence bond metal and superconductivity. *Phys. Rev. Lett*, 91:097003, 2003.

[53] M. M. Maska, M. Mierzejewski, and B. Andrzejewski. Possible singlet to triplet pairing transition in $NaCo_2O_4 \cdot H_2O$. http://arXiv.org/abs/cond-mat/0312174.

[54] G. Burns. *High-temperature suerconductivity.* Academic press, Inc., 1250 Sixth Avenue, San diego, CA 92101, 1992.

[55] H. Sakurai, K. Takada, and S. Yushii. Unconventional upper and lower critical fields and normal state magnetic susceptibility of the novel superconducting compound $NaCo_2O_4 \cdot H_2O$. http://arXiv.org/abs/cond-mat/0304503.

[56] P. Badica, T. Kondo, K. Togano, and K. Yamada. Evidence of large anisotropy in the magnetization of $NaCo_2O_4 \cdot H_2O$ quasi single crystal superconductor. http://arXiv.org/abs/cond-mat/0402235.

[57] The four point electrical probe, 2003. http://www.users.qwest.net/ csconductor/Experiment_Guide/Four20Po.

[58] W. R. Beam. *Electronics of solids.* McGraw-Hill, New York St. Louis San Fransisco Toronto London Sydney, 1965.

[59] T. Roch. Study of colossal magnetoresistance and pressure effects in $la_{2/3}ca_{1/3}mno_3$ thin films. M.sc. physics thesis, Department of Physics, Brock University, 1998.

[60] J. L. Lou, N. L. Wang, and G. T. Liu. Metamagnetic transition in $Na_{0.85}CoO_2$ single crystals. http://arXiv.org/abs/cond-mat/0404432, 2004.

[61] J. Wooldridge, D. Mc Paul, G. Balakrishnan, and M. R. Lees. Investigation of the spin density wave in Na_xCoO_2. *J. Phys:Condensed Matter*, 17:707–718, 2005.

[62] H. Kishan, M. A. Ansari V. P. S. Awana, A. Gupta, and R. B. Saxena. Resistivity and thermoelectric power of Na_xCoO_2(x=1, 0.7 and 0.6) system. *J. Appl. Phys. MMM*, pages BS–14, 2004.

[63] T. Motohashi, M. Karppinen, and H. Yamauchi. Electromagnetic and thermoelectric characteristics of Na_xCoO_2 of precisely controlled Na nonstochiometry. *Mat. Res. Soc. Symp. Proc*, 755:D11.17.1–6, 2003.

[64] M. Eremets. *High pressure experimental methods.* Oxford science publications, Oxford, 1996.

[65] H. Ploczek. M.sc. physics thesis, Department of Physics, Brock University, 2003.

[66] Aloys Eiling. Ph.d. physics thesis, Department of Physics, Ruhr University, Bochum, 1980.

[67] S. Y. Jacob. Systematic studies of the effect of pressure on magnetic and electronic properties of $la_{2/3}ca_{1/3}mno_3$ thin films with various thickness. M.sc. physics thesis, Department of Physics, Brock University, 1999.

[68] K. Fujita, T. Mochida, and K. Nakamura. High-temperature thermoelectric properties of Na_xCoO_2 single crystal. *J. Appl. Phys.*, 40:444–4647, 2001.

[69] Y. Wang, N. S. Rogado, R. J. Cava, and N. P. Ong. Anomalous high temperature Hall effect on the triangular lattice $NaCo_xO_2$. http://arXiv.org/abs/cond-mat/0305455.

[70] Q. Huang, M. L. Foo, R. A. Pascal, J. W. Lynn, B. H. Toby, Tao He, H. W. Zanbergen, and R. J. Cava. Coupling between electronic and structural degrees of freedom in the triangular lattice conductor $NaCo_xO_2$. http://arXiv.org/abs/cond-mat/0406570.

[71] S. P. Bayrakci, C. Bernhard, D. P. Chen, B. keimer, R. K. Kremer, P. Lemmens, C. T. Lin, C. Niedermayer, and J. Strempfer. Bulk antiferromagnetism in $Na_{0.82}CoO_2$ single crystals. *Phys. Rev. B*, 69:R100410, 2004.

[72] E. Fawcett, H. L. Albert, V. Y. Galkin, D. R. Noakes, and J. V. Yakhmi. Spin-density-wave antiferromagnetism in chromium alloys. *Rev. Mod. Phys.*, 66:25, 1994.

[73] J. Sugiyama, C. Xia, and T. Tani. Anisotropic magnetic properties of $Ca_3Co_4O_9$: Evidence for a spin-density-wave transition at 27 k. *Phys. Rev. B*, 67:104410, 2003.

[74] M. Bruhwiler, B. Batlogg, S. M. Kazakov, and J. Karinski. Evidence for two electronic components in Na_xCoO_2(x=0.7-0.75). http://arXiv.org/abs/cond-mat/0309311, 2003.